UNIVERSITY OF THESSALY

SCHOOL OF ENGINEERING

DEPARTMENT OF MECHANICAL ENGINEERING

DESIGN OF SPUR GEARING USING AGMA STANDARD. VERIFICATIONG WITH FINITE ELEMENT ANALYSIS [FEA].

by

FOTIADIS KIRIAKOS-PASCHOS IOANNIS

Submitted in partial fulfillment of the requirements for the degree of Diploma in Mechanical Engineering at the University of Thessaly

Volos, 2020

UNIVERSITY OF THESSALY

SCHOOL OF ENGINEERING

DEPARTMENT OF MECHANICAL ENGINEERING

DESIGN OF SPUR GEARING USING AGMA STANDARD. VERIFICATIONG WITH FINITE ELEMENT ANALYSIS [FEA].

by

FOTIADIS KIRIAKOS-PASCHOS IOANNIS

Submitted in partial fulfillment of the requirements for the degree of Diploma in Mechanical Engineering at the University of Thessaly

Volos, 2020

Approved by the Committee on Final Examination:

Advisor	Dr. Karamanos Spyros, Professor, Department of Mechanical Engineering, University of Thessaly
Member	Dr. Kermanidis Alexis, Associate Professor, Department of Mechanical Engineering, University of Thessaly
Member	Dr. Sotiria Chouliara, Lab Teaching Personnel, Department of Mechanical Engineering, University of Thessaly

Date Approved: [February 24, 2020]

DESIGN OF SPUR GEARING USING AGMA STANDARD. VERIFICATIONG WITH FINITE ELEMENT ANALYSIS [FEA].

FOTIADIS KIRIAKOS-PASCHOS IOANNIS

Department of Mechanical Engineering, University of Thessaly

Supervisor: Dr Spyros Karamanos

Abstract

The goal of this paper is to examine a generalized designing procedure for spur gears and achieve verification by using a finite elements analysis software. In the beginning it is crucial that the basic characteristics of the spur gears are clarified, as well as the AGMA criterion, so the reader would be able to understand the procedure that is going to be followed. Afterwards, a reference about usual failure modes resulting from excessive contact and bending stress is comprehensively represented. Subsequently, the main topic of this thesis is taking place and the first action is the drawing of the gears, then the construction of the finite element analysis model and finally the observation and discussion of the results.

Table of Contents

1 INTRODUCTION 7

2 CHAPTER 2 SPUR GEAR BASICS 8

2.1 USES AND CHARACTERISTICS OF GEARS 8
2.2 SPUR GEARS TOOTH PROFILE AND GEOMETRY 8
2.2.1 Geometry Parameters 9
2.2.2 Tooth Generation 11
2.2.3 Interference 13
2.3 FAILURE MODES 14
2.3.1 Pitting 14
2.3.2 Wear 16
2.3.3 Breakage 19
2.4 FORCE ANALYSIS ON SPUR GEARING 20
2.5 LEWIS EQUATION FOR TOOTH BENDING STRESS 22
2.6 GEAR DESIGN USING AGMA EQUATION 23
2.6.1 Overload Factor, K_o 25
2.6.2 Dynamic factor, K_v 25
2.6.3 Size factor, K_s 26
2.6.4 Load distribution factor, K_H 26
2.6.5 Rim-thickness factor, K_B 28
2.6.6 Bending-Strength Geometry factor, Y_j 29
2.6.7 Surface-Strength Geometry factor, Z_I 30
2.6.8 Surface condition factor, Z_R 31
2.6.9 The Elastic Coefficient, Z_E 31
2.6.10 AGMA strength equations 32
2.6.11 Hardness-Ratio factor, Z_W 33
2.6.12 Reliability factor, Y_Z 34
2.6.13 Temperature factor, Y_θ 34
2.6.14 Stress-cycle factor Y_N 34
2.6.15 Allowable Bending Stress, S_t 36
2.6.16 Allowable Contact Stress, S_c 37
2.6.17 Safety Factors S_F and S_H 38

3 SPUR GEAR DESIGN & DRAWING 39

3.1 CASE STUDY 39
3.2 AGMA RESULTS 39
3.2.1 Calculation of computed data 42
3.2.2 Calculation of Bending stress 43
3.2.3 Calculation of contact stress 45
3.2.4 Allowable bending stress 46

3.2.5 Allowable contact stress *47*
3.2.6 Safety factors *48*
3.3 SPUR GEAR DRAWING IN SOLIDWORKS (CAD) 49
3.3.1 Modeling parameters *49*
3.3.2 Spur gear and pinion drawing *51*
3.3.3 Assembly *57*
3.3.4 Simplified geometry for Finite Element Analysis *59*
4 FE MODELLING (ABAQUS)-PREPARATION OF THE MODEL 60
4.1 ABAQUS MODEL INITIATION 61
4.2 MATERIAL DEFINITION 61
4.3 INTERACTION PROPERTIES 62
4.4 ANALYSIS STEPS-BOUNDARIES AND LOAD CONDITIONS 64
4.5 MESH SELECTION 64
5 FEA RESULTS AND AGMA STANDARD COMPARISON 69
5.1 BENDING STRESS COMPARISON 69
5.1.1 Errors between AGMA and FEA *70*
5.1.2 Safety Factors *71*
5.2 CONTACT STRESS COMPARISON 72
5.2.1 Errors between AGMA and FEA *73*
5.2.2 Safety factors *73*
6 CONCLUSION 74

1 Introduction

Gears are the most commonly used machine elements in power transmission applications. They are basically used for decreasing or increasing the rotational velocity and the magnitude of a power source. There are countless fields in which gears are necessary, so optimizing the efficiency, the operational quality and their durability while minimizing the cost, would escalate the global profit. In order to achieve that, ways to improve the designing of the gears are still an open field. The most commonly adopted standards for gear design are ISO and AGMA (American Gear Manufacturers Association) Standards. Another way is using FEA (Finite Elements Analysis), in this thesis a comparison between stress analysis results from AGMA and FEA is going to be reviewed.

Similar work has been represented from Seok-Chul Hwang **[8]** , where FEA model contact stress results are compared with the ones extracted from the AGMA criterion, however there are major differences in the finite element analysis procedure that is going to be applied in the following thesis. Briefly said, Hwang divided the problem in ten different cases, where the driving gear was kept fixed in every case, while the driven one had a moment applied on it and each time the contact position was changed to cover a whole tooth contact cycle. The FE method selected was proposed by Rhys Gareth Jones **[10]** , where the problem was devided in three steps known as the contact, load and rotation step. In the end the extracted contact and bending stress results from the FEA software are compared with the corresponding ones from the AGMA standard. The software that was chosen is ABAQUS, which is a software application for modeling and analyzing mechanical components under certain loads and boundaries conditions. In addition, it provides visualization choices from the finite element analysis. In the preprocessing the gears are drawn in SOLIDWORKS, which is a CAD software.

2 Chapter 2 Spur Gear Basics

2.1 Uses and Characteristics of Gears

Gears are the most popular mechanical members in power transmission cases. They transfer rotary motion from one shaft to another with high efficiency reaching up to 98%. However, the manufacturing cost is higher than this of chains and belts (devices used for the same purpose) and it varies depending on the constructing precision. Additionally, due to their durability and roughness they provide a lasting and maintenance-free life function.

The most common failure modes in gears are fatigue fracture due to bending stress in the root of the tooth and wear of the surface caused by the contact stress between the meshing gears, those two parameters are determinant for designing a gear. A reliable standard concerning the design, analysis and geometric characteristics of the teeth in gearing is the American Gear Manufacturers Association (AGMA).

2.2 Spur Gears Tooth Profile and Geometry

The main types of gearing are spur, helical, bevel and worm gears. For the purpose of this thesis spur gears will be studied using finite elements analysis and comparing with the corresponding AGMA standard. Spur gears are the most popular among the family of gears, they are simple and easy to be constructed combining high efficiency. Their teeth are parallel to the rotation axis and the load is being transferred from one shaft to another parallel shaft.

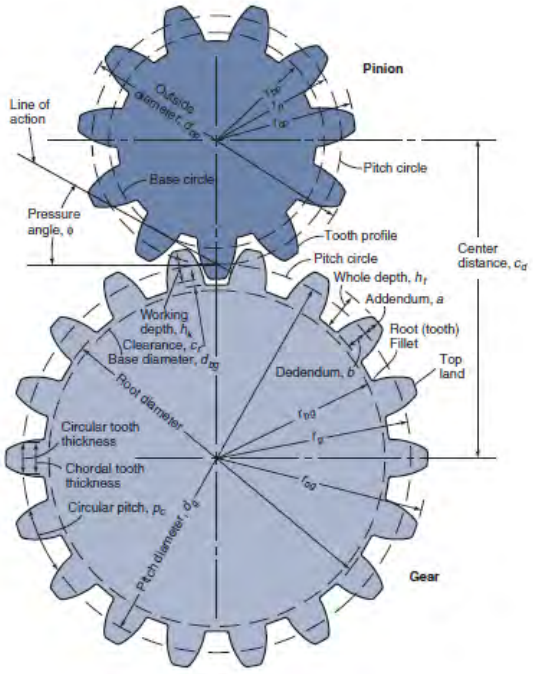

Figure 2.1 Basic spur gear geometry [2]

2.2.1 Geometry Parameters

Before the beginning of the analysis of the gear meshing some important geometric parameters of the gear and the gear tooth must be defined. Pinion is the driving gear, namely the one that transfers the load and it is usually smaller in size and teeth number than the driven gear, the one that receives the driving force. In **Figure 2.1** are depicted the basic geometrical characteristics of the pinion and the gear.

Center distance (c_d) is calculated as:

$$C_d = \frac{d_p + d_g}{2} \quad [2.1]$$

where d_p stands for the diameter of the pinion and d_g for the diameter of the gear, and it is the distance between the two axes of rotation.

Circular pitch (p_c):

$$p_c = \frac{\pi d}{N} = \frac{\pi d_p}{N_p} = \frac{\pi d_g}{N_g} \quad [2.2]$$

It's the range on the pitch circle, beginning from one tooth and ending on a point in a neighboring one. N_p and N_g stand for the number of the teeth for the pinion and the gear respectively. The **gear ratio (g_r)** can be computed and is expressed as:

$$g_r = \frac{d_g}{d_p} = \frac{N_g}{N_p} \quad [2.3]$$

One of the most important characteristic is the **module (m)** and it's the ratio of the pitch diameter to the number of teeth and the basic requirement between the two meshing gears is that they have the same module.

$$m = \frac{d_g}{N_g} = \frac{d_p}{N_p} \quad [2.4]$$

Preferred	1, 1.25, 1.5, 2, 2.5, 3, 4, 5, 6, 8
	10, 12, 16, 20, 25, 32, 40, 50
Allowed	1.125, 1.375, 1.75, 2.25, 2.75, 3.5, 4.5
	5.5, 7, 9, 11, 14, 18, 22, 28, 36, 45

Table 2.1 Preffered and allowed module values

In **Table 2.1** the preferred and allowed values of module for spur gears are represented. Modules less than one are used in specific cases.

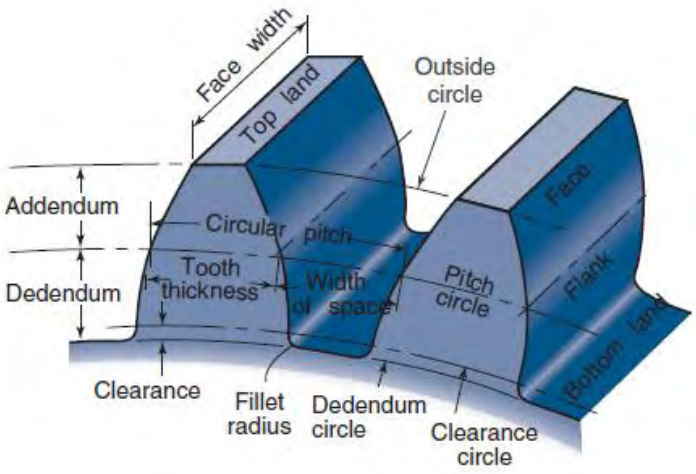

Figure 2.2 Gear teeth nomenclature

As it is shown in **Figure 2.2** **addendum (a)** is measured as the distance between the pitch circle and the top land while **dedendum (b)** is the one from the pitch circle to the bottom land. **Clearance (c)** is quantity by which the dedendum surpasses the addendum. Summarizing, following equation is extracted:

$$c = b - a \qquad [2.5]$$

While knowing those three parameters, other significant geometric characteristics can be computed, for both pinion and gear, such as:

Outside diameter (d_0):

$$d_0 = d + 2a \qquad [2.6]$$

Root diameter (d_r):

$$d_r = d - 2b \qquad [2.7]$$

Total depth (h_t):

$$h_t = a + b \qquad [2.8]$$

Working depth (h_k):

$$h_k = a + a = 2a \qquad [2.9]$$

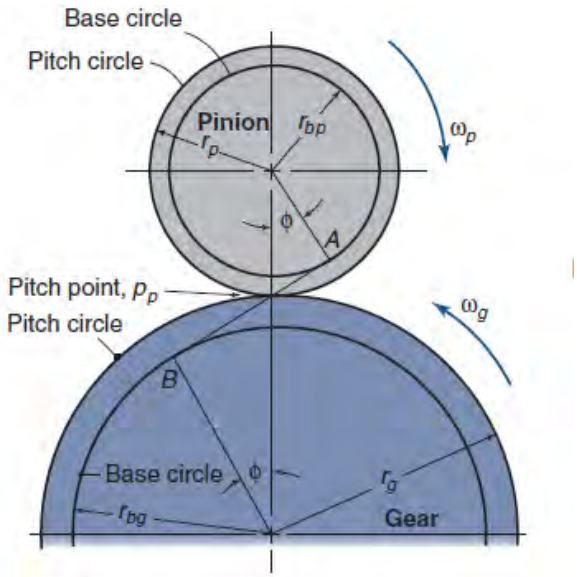

Figure 2.3 ***Pitch and base circles for pinion and gear*** *(Bernard J. Hamrock, 2004)*

Another significant parameter is the **pressure angle(φ)** shown in **Figure 2.3**: it's the angle between the line that connects the two centers and a vertical one to the line of action and it varies between 20˚and 25˚. On the line of action, the tooth connection takes place during the contact procedure. Also, the following equation is easily extracted for both pinion and gear:

$$r_b = r\cos\varphi \qquad [2.10]$$

where r_b is the radius of the base circle.

2.2.2 Tooth Generation

It is necessary for the mating teeth and especially their surfaces to have conjugate action, meaning that there will be a constant angular velocity ratio between the two gears. Using the **involute profile** smooth rolling motion is achieved, reduction of the operation noise and there will always be at least a couple of teeth in connection during the whole procedure.

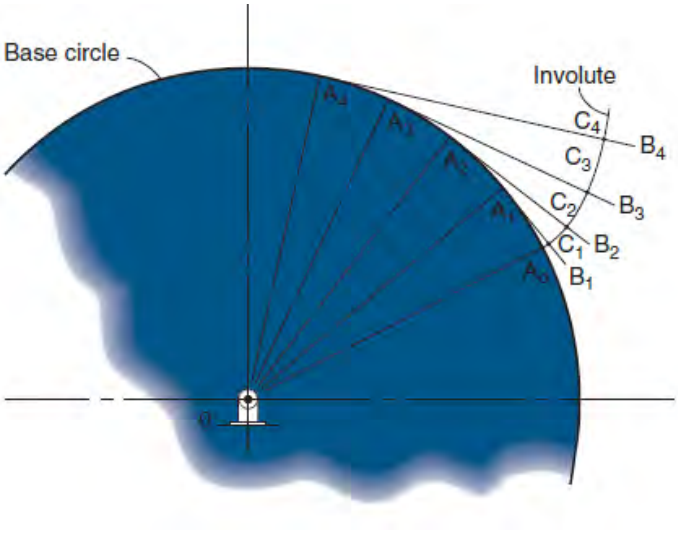

Figure 2.4 Involute curve generation [2]

In **Figure 2.4** the generation of the involute curve is pictured and it consists of the following steps**[2]**:

1. Separation of the base circle in equal partitions A_0, A_1, A_2, A_3, A_4, …
2. With starting point A_1 a straight line A_1B_1 is drawn, vertical to the radius $0A_1$. The same procedure goes for A_2, A_3, …
3. Longways A_1B_1 the distance A_0B_1 is laid off, thus creating C_1. The same goes for A_2B_2 where twice the distance is laid off, thus creating C_2 etc.
4. Generate the involute curve using A_0, C_1, C_2, C_3, …
5. The curve has its starting point on the base circle and it reaches the outside circle. A fillet transition is applied between the dedendum and the addendum circles.

However, to obtain smooth rolling and constant teeth touch, it is necessary for one pair of teeth to be connected at the very time another pair is losing contact. This state is expressed by **contact ratio(C_r)**, which is actually the definition of the average number of teeth paired at the same time.

Contact ratio:

$$C_r = \frac{L_{ab}}{p_b} = \frac{L_{ab}}{p_c \cos\varphi} \qquad [2.11]$$

L_{ab} stands for the **length of action** which is a line where the contact of the connecting pair is taking place.

Length of action:

$$L_{ab} = \sqrt{r_{op}^2 - r_{bp}^2} + \sqrt{r_{og}^2 - r_{bg}^2} - c_d \sin\varphi \qquad [2.12]$$

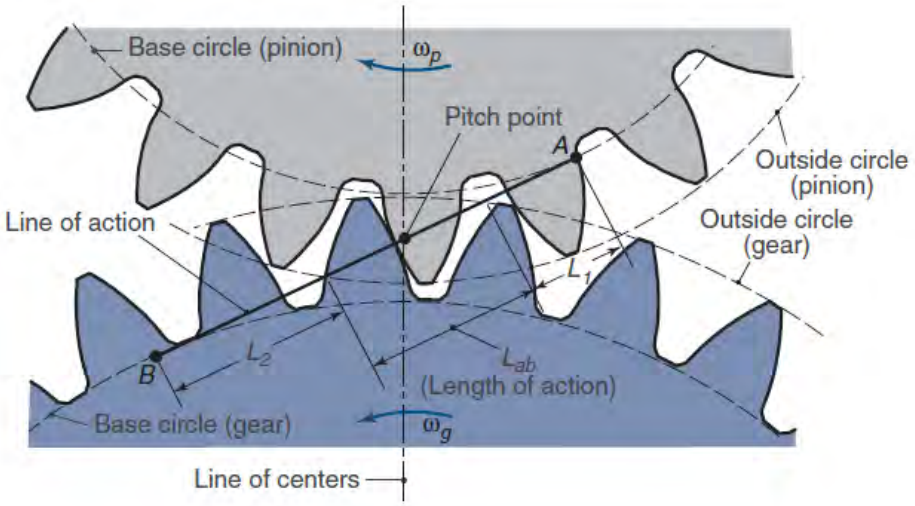

Figure 2.5 Details on line and length of action

While $\mathbf{p_b}$, just like $\mathbf{p_c}$, is the **base pitch**, meaning the distance measured on the base circle from one point on the tooth to the neighboring one on the other tooth. Having a contact ratio equal to 1 means that when teeth connection occurs the previous pair loses contact at the same time. Values greater or equal to 1.2 are recommended to avoid poor performance, extra vibration, noise and backlash. Also. Reduction of stresses is achieved because the load is shared between two pairs of mating teeth.

2.2.3 Interference

Contact occurs when the connection between the tip of the gear and the flank of the pinion takes place. Interference is when non-conjugate parts of the mating teeth are connecting. In this case the first point of the pinion flank that connects, is below the base circle, which is a non-involute portion of the teeth. The problem is that the involute portion of the gear tends to interfere with a non-involute one of the pinion. If the manufacturing of the gears is made with generation methods, the interference problem is dealt with the undercutting effect, meaning that the cutting tool abstracts the parts of the flank that interfere. However, this method weakens the teeth and it is not desirable. Interference problems should be avoided during the design and for that purpose the minimum number of pinion teeth and the maximum number of gear teeth are computed as:

$$N_P = \frac{2k}{(1+2m)(\sin\varphi)^2}\left(m+\sqrt{m^2+(1+2m)(\sin\varphi)^2}\right) \qquad [2.13]$$

Where k is 1 for full-depth teeth and 0.8 for stub teeth. Stub teeth gears have a working depth near 20% less than the full-depth ones.

The number of the teeth of the gear can be expressed for a certain non-interference pinion:

$$N_G = \frac{N_P^2 \left(\sin\varphi\right)^2 - 4k^2}{4k - 2N_P \left(\sin\varphi\right)^2} \qquad [2.14]$$

2.3 Failure Modes

Another significant field which must be discussed is the failure modes that can be developed during the lifetime of a conjugate action of gears and ways to avoid or correct them. They are divided in two main categories due to the cause of their formation. As said in the beginning of this chapter the main failure modes are fatigue fracture due to bending stresses and wear of the surface caused by contact stresses.

2.3.1 Pitting

Pitting is a form of surface fatigue that occurs when the stresses on the surface are repeatedly exceeding the endurance limit of the material, where endurance limit is the maximum stress under which the material can possibly withstand an infinite amount of cycles. Its divided in tree main types:

- Initial pitting
- Destructive pitting
- Normal pitting

Initial pitting (**Figure 2.6**) initiates from stress concentrations on abnormalities on the flank surface of the tooth around the pitchline area and the development of the phenomenon is relatively fast. For through-hardened gears no correction is needed (most of the times) and is common and normal phenomenon. However, there are ways to remediate or prevent this form of failure, such are:

- Pitting reduction by using tooth finishing tools
- Insignificant drop of the load and speed
- Teeth are copper or silver plated to avoid or decrease initial pitting.

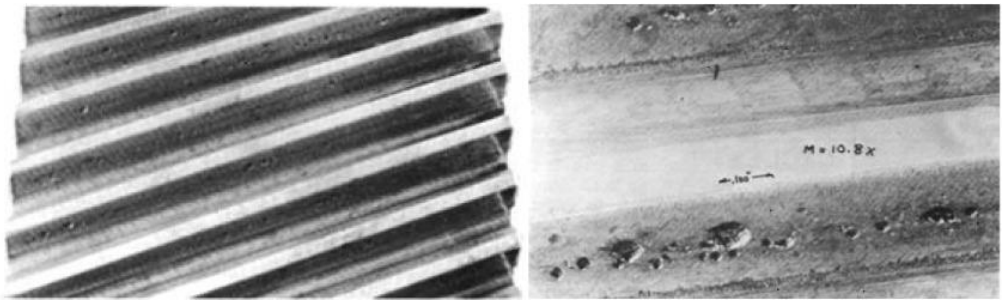

Figure 2.6 (a) Initial pitting (b) Enlarged photo [3]

Destructive pitting (**Figure 2.7**) is usually located in the dedendum part of the tooth and it grows bigger and bigger in size and number of pits as time passes by. Destructive pitting is the output from high load conditions and the predomination of initial pitting.

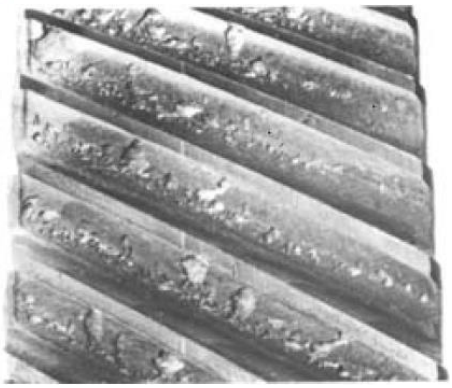

Figure 2.7 Destructive pitting in a through hardened gear [3]

The severeness is equal to the one of the initial pitting at the beginning of the occurrence, however it progressively surpasses it, resulting to the complete destruction of the surface. The following **Figure 2.8** compares the severity of the progressive pitting with the one of the initial as function of the cycles.

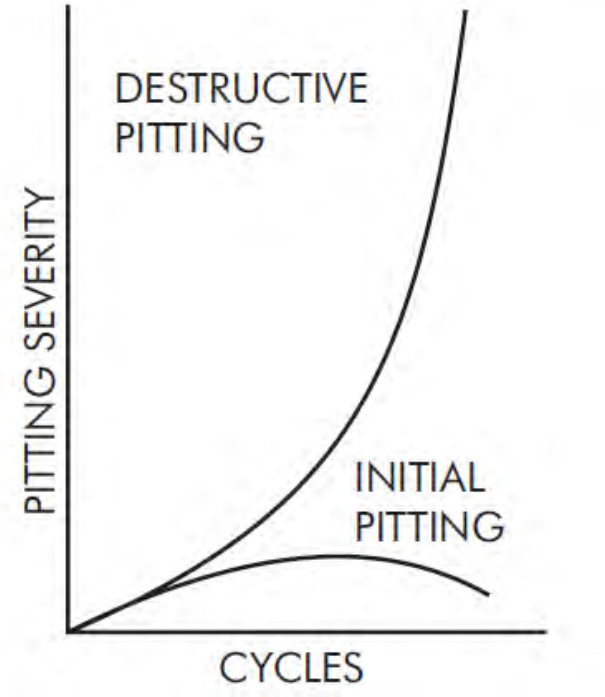

Figure 2.8 Comparison of pitting severity [3]

Normal dedendum pitting (**Figure 2.9**) occurs across the whole dedendum portion of the tooth flank an as the initial pitting it can be confronted. The existence of micro-cracks on the surface, in combination with the lubrication oil are the main cause for the initiation of normal pitting. Specifically, the oil is being trapped in the micro-cracks and with the application of the contact stress, the recesses are being stretched by the increase of the hydraulic pressure inside them, resulting in the creation of a pit.

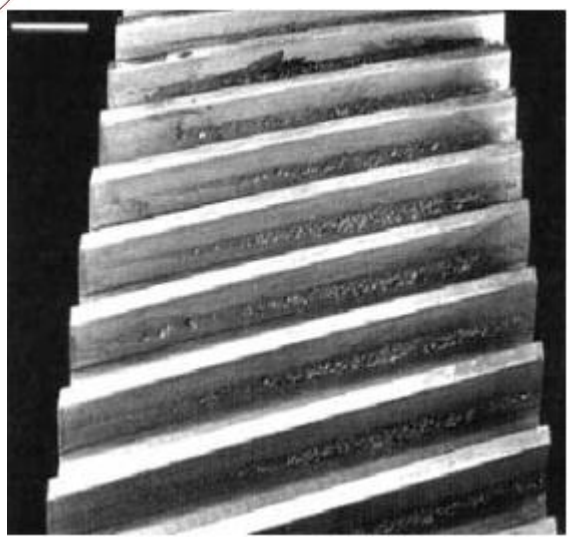

Figure 2.9 Normal dedendum pitting [3]

2.3.2 Wear

Wear is a general term describing the loss of material on the contacting portion of the tooth flank. Its divided in two main types, abrasive and adhesive wear.

Abrasive wear takes place when hard particles are trapped between the teeth and slide under pressure. Such are dirt, sand or metal parts and they can be imported by the lubricant mean. The surface print resembles to scratches as shown in the following figure and this form of abrasive wear is called scratching.

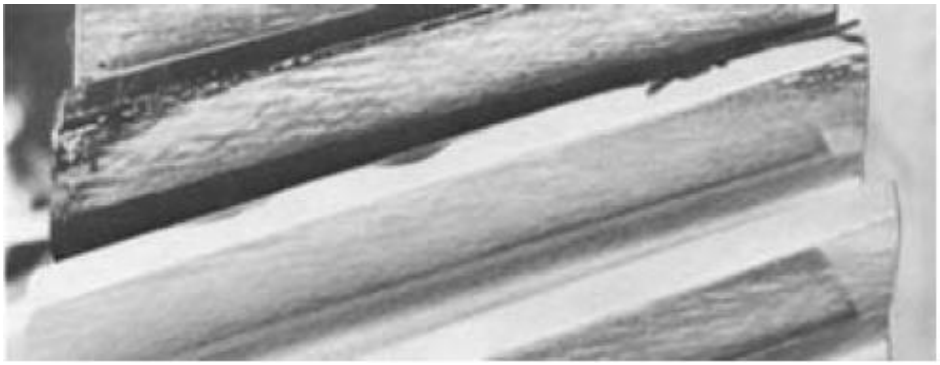

Figure 2.10 Scratching [3]

Adhesive wear (see **Figure 2.11**) results from high magnitude of the attraction forces of the atoms from the two contacting surfaces and it depends on the physical chemistry of the materials in contact and the lubricant that is being used. The bonding between the two surfaces grows bigger until a part is detached resulting to a wear particle formation.

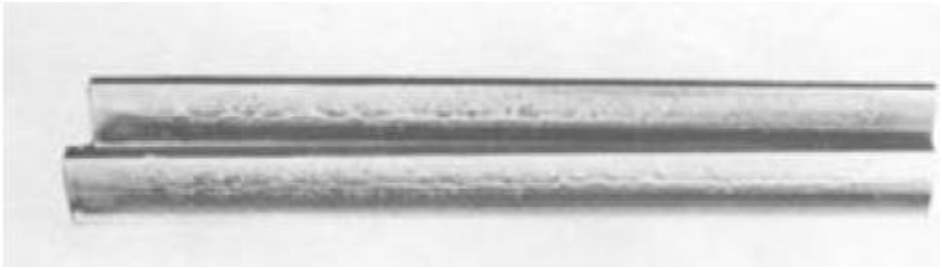

Figure 2.11 Adhesive wear through hardened gear [3]

Considering the degrees of wear, there are three of them:

- Light
- Moderate
- Excessive

Light wear is a normal condition for the gears and its effect on the performance is insignificant. It usually appears in low speed applications in both abrasive and adhesive applications.

Moderate wear will affect gear performance in its expected life. As it is shown the progress of moderate wear in **Figure 2.12**, there is material loss from the whole portion but especially around the dedendum area. The tolerance in moderate wear depends on the requirements of the application. The main cause for this phenomenon is the lubrication, thus in most cases no correction is needed than the condition of the lubricant.

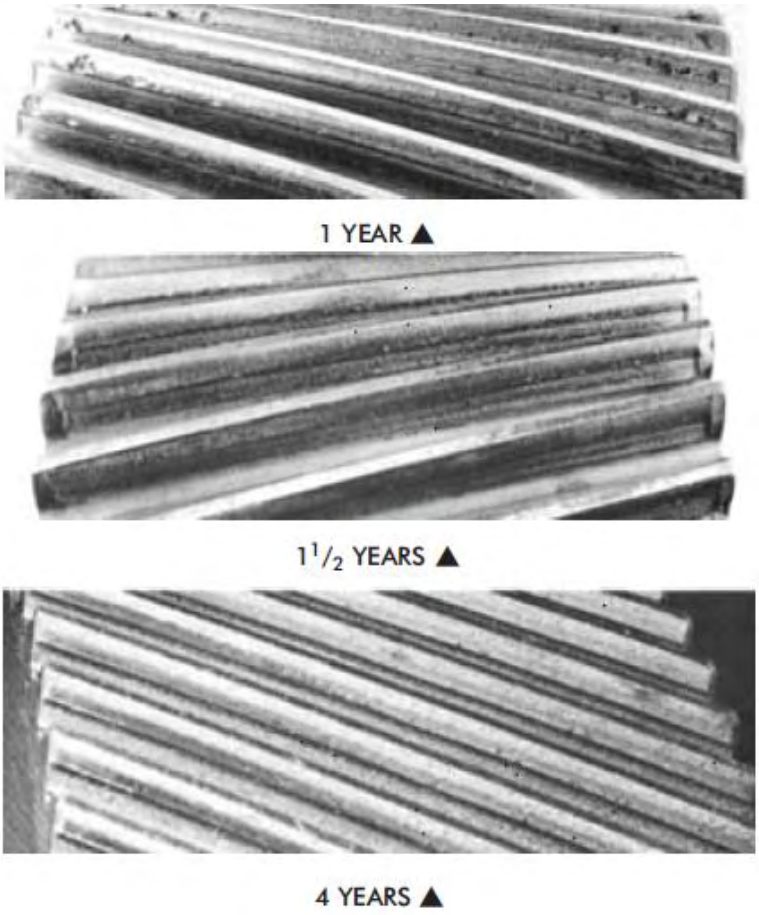

Figure 2.12 Early occurrence of moderate wear [3]

Excessive wear completely changes the tooth surface, resulting in shorting gear's life leading to breakage. Development of such wear comes from overloading, polluted lubricant and wrong oil selection (low viscosity) depending always on the working parameters.

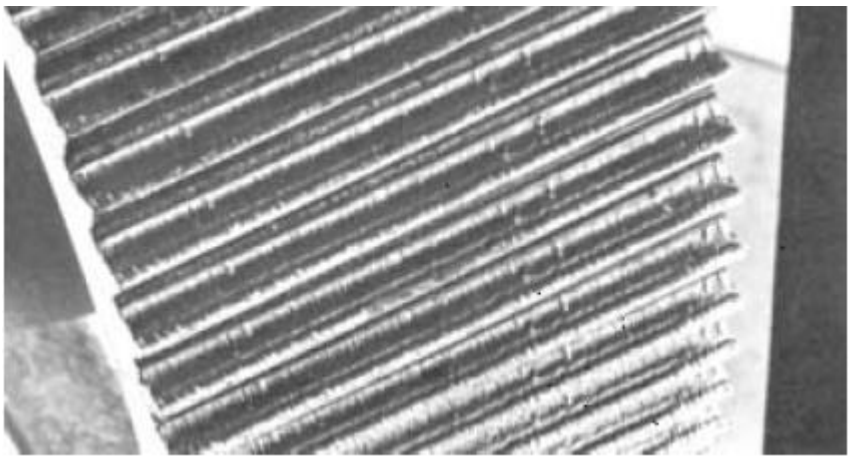

Figure 2.13 Excessive wear [3]

2.3.3 Breakage

Breakage is the terminal form of failure and is basically caused by bending stresses which are the most powerful ones acting on the gear. It is common for the rotation of the gears to be one-way, so is the bending load reaching its maximum at the root of the tooth causing fatigue failure after a quiet big number of cycles. The existence of cracks in the root initiates the phenomenon and leads to the final fracture of the tooth (see **Figure 2.14**). Breakage can also result from overloading. Low cycle fatigue is caused either from a small number of high loads cycles or from a decisive single high load and the result is the complete failure of the flank.

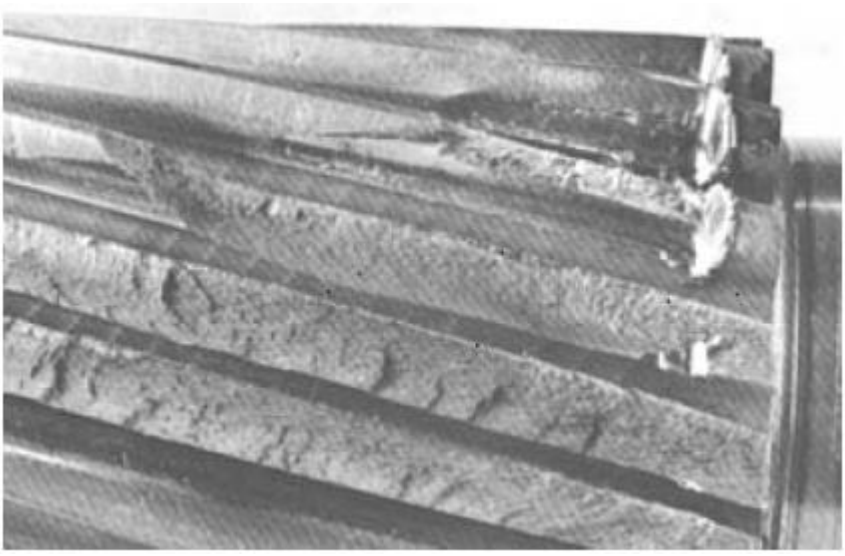

Figure 2.14 Low cycle fatigue [3]

The most usual fatigue breakage mode is the classical tooth root fillet fatigue fracture. The orientation of the crack is at the fillet of the tooth's root. The progress is fueled when tensile stresses surpass the endurance strength of the material. Its easily detected, as all fatigue failure cases, from the existence of the "beach marks" which are deferent height levels of material resembling to the traces that are left behind from the tide on the beach (**Figure 2.15**).

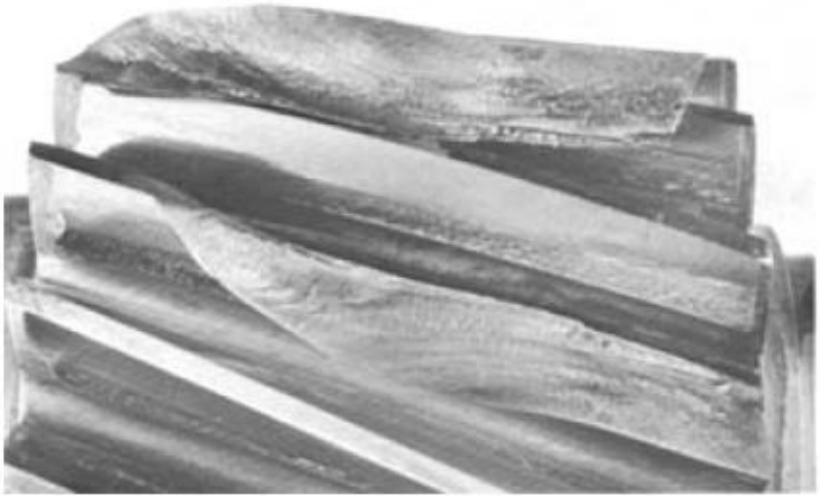

Figure 2.15 Tooth fracture (root fillet fatigue) [3]

2.4 Force analysis on spur gearing

When investigation of the occurring forces on the gears is needed, first of all a free body diagram is being constructed. Before beginning the force analysis, it shall be mentioned that the letters a, b designate the shafts of the pinion and gear respectively, also the numbers 1, 2 designate the pitch circle of pinion and the gear. With this notation, the reference of the force exerted from the gear (2) to the pinion (1) is F_{21}. Also, the torque exerted from the shaft (α) to the pinion (2) is $T_{\alpha 1}$. The letter φ refers to the pressure angle and the diagonal line is the pressure line. N_1 and n_2 refer to the pinion and the gear speed (rev/min). Now everything is ready for the examination.

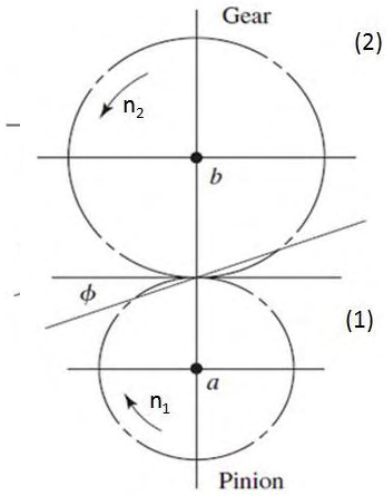

Figure 2.16 Force and torque analysis on the pinion

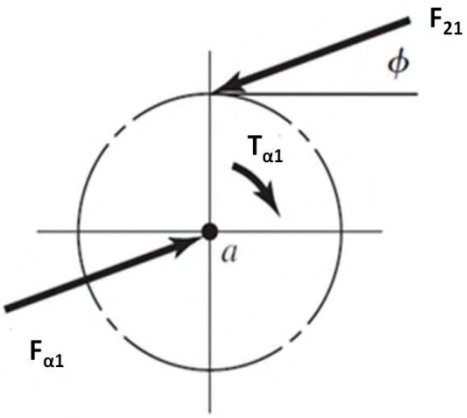

Figure 2.17 Revolution of pinion and gear

When the pinion drives the gear there are action and reaction forces. The reaction forces of the mating teeth occur along the pressure line. When the pinion pushes the gear, the gear pushes it back, so the reaction force is supposed to be at the top land of the pinion pitch circle (F_{21}). F_{21} has a certain angle which is the pressure angle as it is mentioned in **Figure 2.17**. F_{21} can be decomposed to a horizontal and a radial force.

$$F_{21}^{t} = F_{21} \cos\varphi \qquad [2.15]$$

$$F_{21}^{r} = F_{21} \sin\varphi \qquad [2.16]$$

The tangential load is the only load from which useful relations can be obtained, the radial component serves no meaningful purpose. The horizontal force is also called *transmitted load*. In order to balance the pinion there has to be a force in the opposite direction of F_{21}. That force is counterbalanced by the shaft and occurs at the center of the pitch line circle, at point α. There is one more problem, F_{21} is also generating torque. So the shaft also provides torque (T_{a1}) to the pinion and the equilibriums of forces and moments are satisfied.

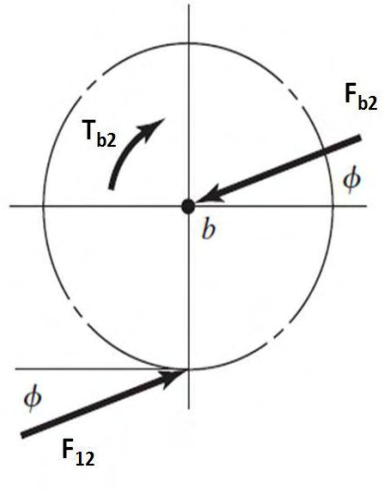

Figure 2.18 Force and torque analysis on the gear

Using a similar approach, by drawing the free body diagram of the gear shown in the **Figure 2.18**. The similar but with different directions. It is obvious that the applied torque and the transmitted load are related to each other by the equation:

$$\mathbf{T_{a2} = \frac{d_p}{2} F_{32}^{t}} \qquad [2.17]$$

Where d_p is the pitch diameter of the pinion. The desired power output of the system can be expressed as:

$$H = T_{a1}\omega \qquad [2.18]$$

Where ω is the radial velocity. The transmitted load is defined as

$$W_t = F_{32}^{t} \qquad [2.19]$$

Transmitted load can be correlated with power through the equation:

$$W_t = \frac{\mathbf{60000}\ H}{\pi dn} \qquad [2.20]$$

Where

$$W_t = transmitted\ load, KN$$

$$H = power, KW$$

$$d = gear\ diameter, mm$$

$$n = speed, rev / min$$

2.5 Lewis equation for tooth bending stress

Wilfred Lewis was an American mechanical engineer graduated from the Massachusetts Institute of Technology in 1875. In the late of 19th century had developed an equation for tooth bending stress. Lewis approached the problem considering the teeth as a rectangular cantilever beam as it is shown in **Figure 2.19**.

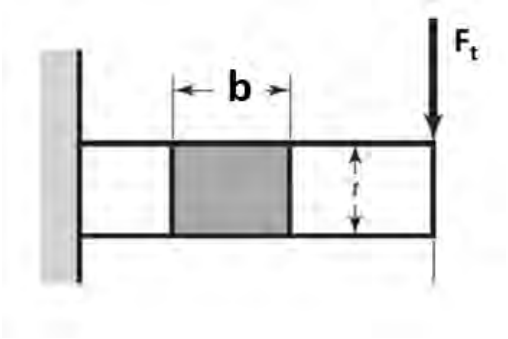

The beam has length l, cross-sectional dimensions F, t and it is applied a load at the edge W_t. Therefore, the bending stress can be expressed as:

$$\sigma = \frac{6F_t l}{Ft^2} \qquad [2.21]$$

Figure 2.19 Gear teeth considered as a beam

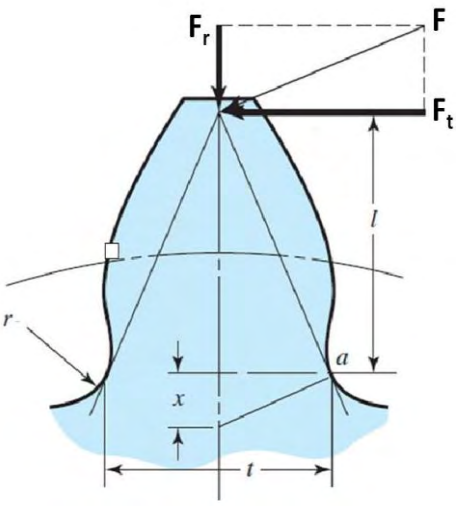

Figure 2.20 Force analysis on a tooth

Referring now to **Figure 2.20**, by similar triangles the following equation is extracted:

$$\frac{t/2}{x} = \frac{l}{t/2} or\ x = \frac{t^2/4}{l} or\ l = \frac{t^2}{4x} \qquad [2.22]$$

Now the bending stress can be expressed as

$$\sigma = \frac{6F_t}{4Fx} \qquad [2.23]$$

And if by multiplying the nominator and the denominator with the circular pitch the tension is as follows:

$$\sigma = \frac{F_t}{Fpy} \qquad [2.24]$$

Letting

$$y = 2x / 3p \qquad [2.25]$$

The final form of Lewis equation is getting by substituting p=πP and y=πY. This gives

$$\sigma = \frac{F_t P}{FY} \qquad [2.26]$$

Where

$$Y = \frac{2xP}{3} \qquad [2.27]$$

Values of Lewis form factor, Y, are obtained from the **Table 2.2** below. These values are for full depth teeth, pressure angle of 20◦ and a P=1 in the plane of rotation.

Number of Teeth	Y	Number of Teeth	Y
12	0.245	28	0.353
13	0.261	30	0.359
14	0.277	34	0.371
15	0.290	38	0.384
16	0.296	43	0.397
17	0.303	50	0.409
18	0.309	60	0.422
19	0.314	75	0.435
20	0.322	100	0.447
21	0.328	150	0.460
22	0.331	300	0.472
24	0.337	400	0.480
26	0.346	Rack	0.485

Table 2.2 Values of Lewis factor considering the number of teeth

2.6 Gear design using AGMA equation

AGMA is an empirical standard which is used in gear design; this empirical model was based mainly on the Lewis equation. The AGMA model can predict if a

gear is safe for use in terms of bending and contact stresses and is commonly used in gear industry.

The fundamental equation for bending stress (SI Units) is:

$$\sigma = F^{'} K_o K_V K_s \frac{1}{b m_t} \frac{K_H K_B}{Y_J} \qquad [2.28]$$

Where

F_t *is the tangential transmitted load*, N

K_o *is the overload factor*

K_V *is the dynamic factor*

K_s *is the size factor*

b *is the face width of the narrower member*, mm

K_H *is the load distribution factor*

K_B *is the rim thickness factor*

Y_J *is the geometry factor for bending strength*

m_t *is the transverse metric module*

The fundamental equation for pitting resistance is:

$$\sigma_c = Z_E \sqrt{F^{'} K_o K_S K_V \frac{K_H}{d_{w1} b} \frac{Z_R}{Z_I}} \qquad [2.29]$$

Where the additional terms are:

$\mathbf{Z_E}$ *is an elastic coefficient*, $\sqrt{\frac{N}{mm^2}}$

$\mathbf{Z_R}$ *is the surface condition factor*

$\mathbf{d_{w1}}$ *is the operating pitch diameter of the pinion*, *mm*

$\mathbf{Z_I}$ *is the geometry factor for pitting resistanse*

2.6.1 Overload Factor, K_o

This factor reflects the degree of non-uniformity of driving and load torques. In real life problems it is not possible to maintain a constant transmitted load over time, so this factor creates an allowance for all externally applied loads. The values of the following **Table 2.3** can be used as a basis for rough estimate. Note that larger values of K_o will yield higher bending stress.

Table of Overload Factors, K_o

	Driven Machine		
Power source	Uniform	Moderate shock	Heavy shock
Uniform	1.00	1.25	1.75
Light shock	1.25	1.50	2.00
Medium shock	1.50	1.75	2.25

Table 2.3 ***Overload factor for various power sources***

2.6.2 Dynamic factor, K_v

The dynamic factor, $\mathbf{K_v}$, is dependent on the linear velocity of the gear. In the **Figure 2.21**the graph of dynamic factor is being shown, based on its linear velocity and Q_v that receives values between 3 and 15 depending on the quality of the gear. These are the equations related to K_v:

$$K_v = \left(\frac{A + \sqrt{200V}}{A} \right)^B \qquad \left[V \; in \frac{m}{s} \right] \qquad [2.30]$$

$$A = 50 + 56\left(1 - B\right) \quad [2.31]$$

$$B = 0.25\left(12 - Q_V\right)^{\frac{2}{3}} \quad [2.32]$$

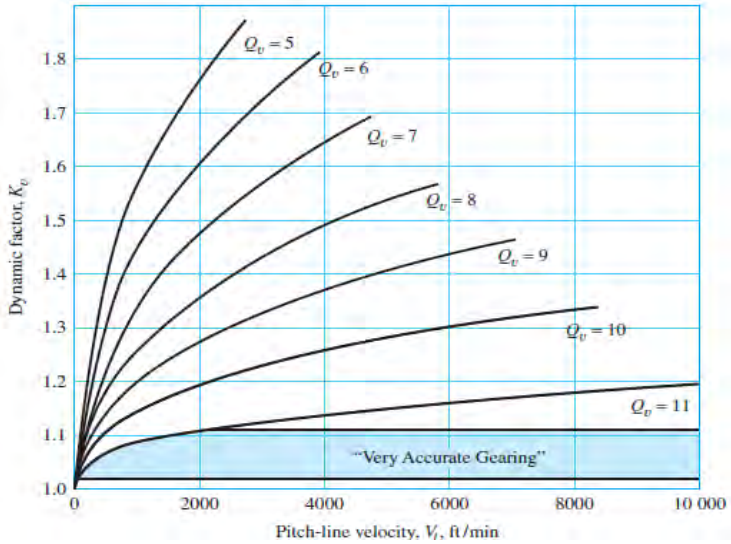

Figure 2.21 Relation between dynamic factor and pitch-line velocity

2.6.3 Size factor, K_s

The size factor expresses how the material properties will react due to the size of the gear. It depends upon the face width (b), the module (m), the Lewis form factor (Y).

$$K_s = \left(0.00155\frac{b\sqrt{Y}}{P_d}\right)^{0.0535} \quad [2.33]$$

Where P_d is the diametral pitch (1/m).

If K_s is less than 1, K_s=1 is chosen.

2.6.4 Load distribution factor, K_H

This factor takes under consideration the non-uniform distribution of the load across the tooth. This factor is due to misalignment between the axes of the shafts or because of the elastic deformation of the gears, shafts and bearings. The analytical equation which gives the load distribution factor is:

$$K_H = 1 + K_{H_{mc}}\left(K_{H_{pf}} K_{H_{pm}} + K_{H_{ma}} K_{H_e}\right) \qquad [2.34]$$

Where

$$K_{H_{mc}} = \begin{cases} 1 & \text{for uncrowned teeth} \\ 0.8 & \text{for crowned teeth} \end{cases}$$

$$K_{H_{pf}} = \begin{cases} \dfrac{b}{10 d_p} - 0.025 & b \le 25.4\ mm \\ \dfrac{b}{10 d_p} - 0.0375 + 0.000492 b & 1 < b < 431.8\ mm \\ \dfrac{b}{10 d_p} - 0.1109 + 0.000815 b - 0.000000353 b^2 & 431.8 < b < 1016\ mm \end{cases}$$

$$K_{H_{pm}} = \begin{cases} 1 & \textit{for straddle - mounted pinion with } S_1 / S < 0.175 \\ 1.1 & \textit{for straddle - mounted pinion with } S_1 / S \ge 0.175 \end{cases}$$

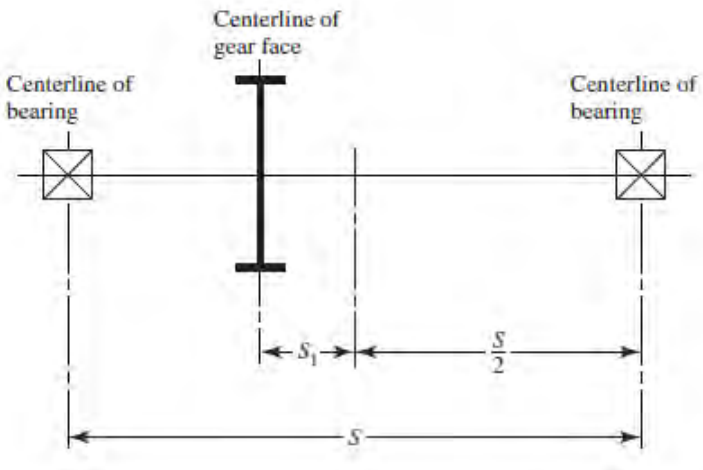

Figure 2.22 Position of the gear and bearings

$$K_{H_{ma}} = A + Bb + Cb^2$$

The values of A, B and C are given in the **Table 2.4**:

Condition	A	B	C
Open gearing	0.247	0.0167	$-0.765(10^{-4})$
Commercial, enclosed units	0.127	0.0158	$-0.930(10^{-4})$
Precision, enclosed units	0.0675	0.0128	$-0.926(10^{-4})$
Extraprecision enclosed gear units	0.00360	0.0102	$-0.822(10^{-4})$

Table 2.4 Constants A, B and C depending on the gear set-up

$$K_{H_e} = \begin{cases} 0.8 \\ 1 \end{cases}$$

for gearing adjusted at assembly, or compatibility is improved by lapping, or both
for all other conditions

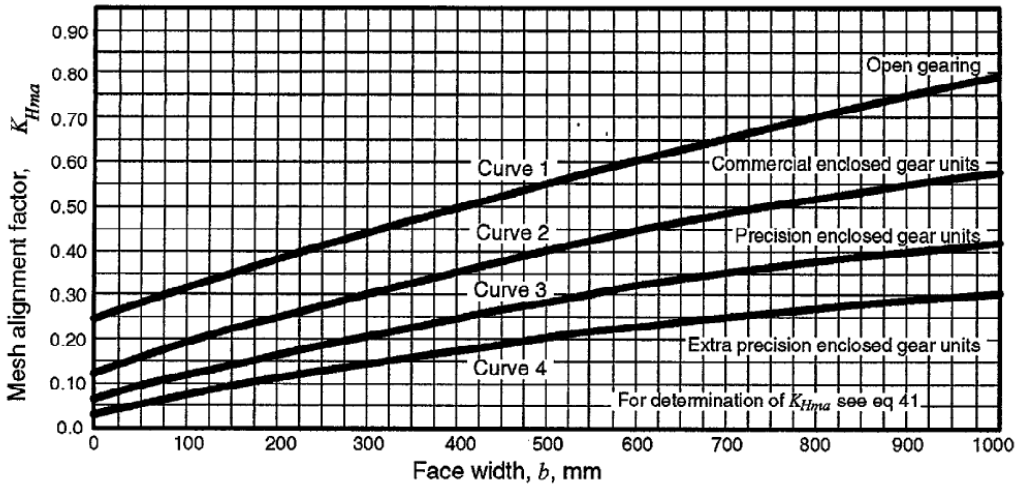

Figure 2.23 Mesh alignment factor 0

2.6.5 Rim-thickness factor, K_B

Rim thickness factor is used when rim thickness is not enough to provide full support for the tooth root. K_B is a function of backup ratio m_B:

$$m_B = \frac{t_R}{h_t} \qquad [2.35]$$

$$K_B = \begin{cases} 1.6 \ln \dfrac{2.242}{m_B} & m_B < 1.2 \\ 1 & m_B \geq 1.2 \end{cases} \qquad [2.36]$$

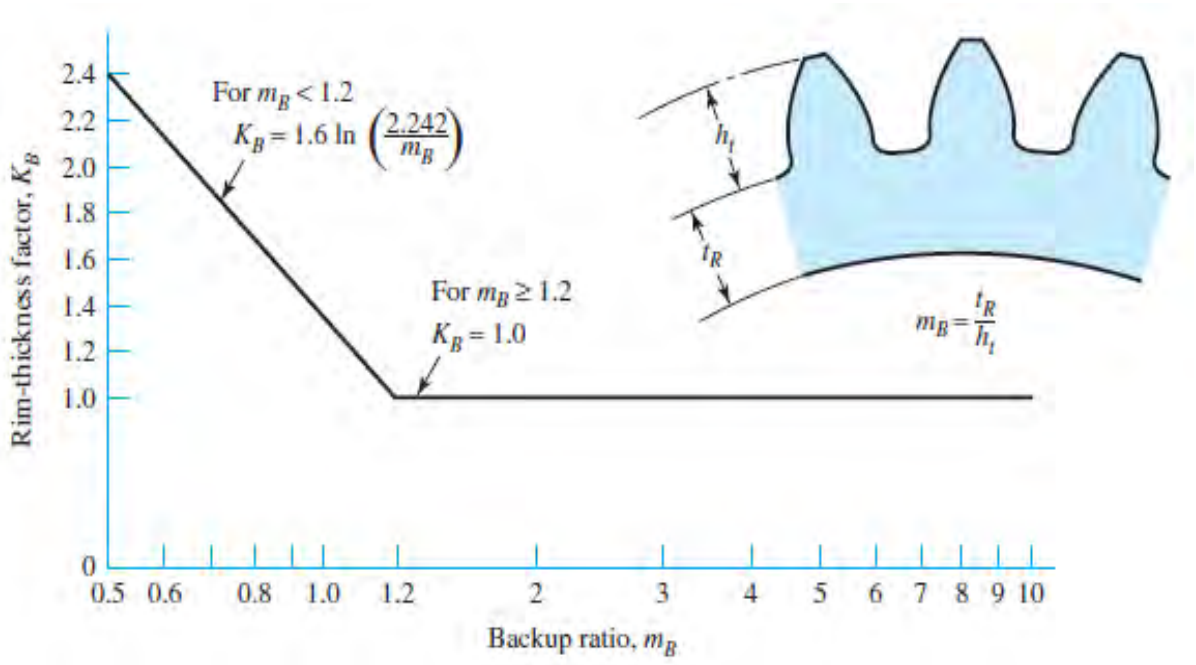

Figure 2.24 Rim thickness factor

2.6.6 Bending-Strength Geometry factor, Y_j

The factor Y_j is a modified Lewis form factor which depends on face-contact ratio, m_F.

$$m_F = \frac{F}{p_x} \qquad [2.37]$$

Where F is the Face width and p_x is the axial pitch. For spur gears m_F=0.

In order to get the factor Y_J, for spur gears, the following **Figure 2.25** is used:

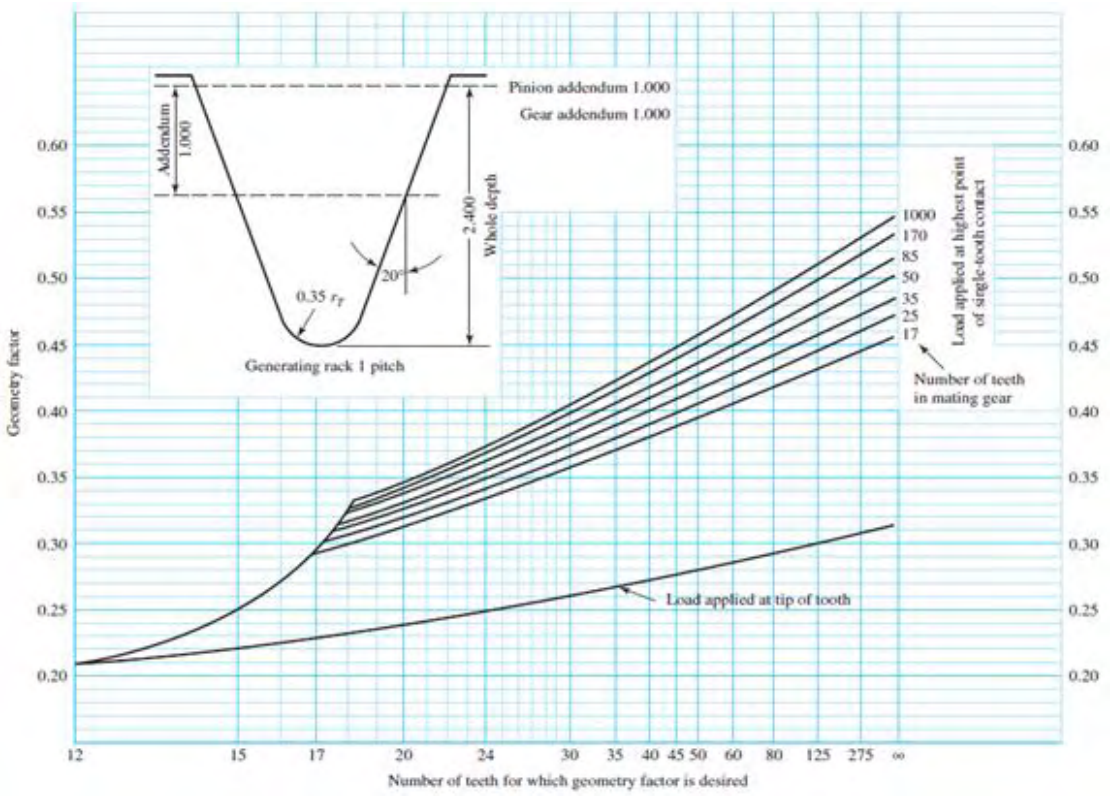

Figure 2.25 Geometry factor Y_j [4]

2.6.7 Surface-Strength Geometry factor, Z_I

Z_I is also called geometry factor for pitting resistance. For spur gears the equation for Z_I is:

$$Z_I = \begin{cases} \dfrac{\cos\varphi \sin\varphi}{2} \dfrac{m_G}{m_G + 1} & \text{For external gears} \\ \dfrac{\cos\varphi \sin\varphi}{2} \dfrac{m_G}{m_G - 1} & \text{For internal gears} \end{cases} \quad \textbf{[2.38]}$$

Where m_G is the gear ratio $m_G = \dfrac{N_g}{N_p} = \dfrac{d_g}{d_p}$.

2.6.8 Surface condition factor, Z_R

This factor exists only in pitting resistance equation. The values it gets depends on:

- The surface quality from cutting,
- shaving,
- lapping, from residual stress and from plastic effects.

When there is a defect on the surface of the gear, Z_R gets a value greater than unity.

2.6.9 The Elastic Coefficient, Z_E

The elastic coefficient is obtained by the equation:

$$Z_E = \left[\frac{1}{\pi \left(\frac{1-\nu_P^{\,2}}{E_P} + \frac{1-\nu_G^{\,2}}{E_G} \right)} \right]^{\frac{1}{2}} \qquad [2.39]$$

Where E is the Young's Modulus and ν is the Poisson's ratio of pinion and gear respectively.

Z_E is also obtained, from the **Table 2.5**.

Elastic Coefficient C_p (Z_E), $\sqrt{\text{psi}}$ ($\sqrt{\text{MPa}}$) *Source: AGMA 218.01*

Pinion Material	Pinion Modulus of Elasticity E_p psi (MPa)*	Gear Material and Modulus of Elasticity E_G, lbf/in² (MPa)*: Steel 30×10^6 (2×10^5)	Malleable Iron 25×10^6 (1.7×10^5)	Nodular Iron 24×10^6 (1.7×10^5)	Cast Iron 22×10^6 (1.5×10^5)	Aluminum Bronze 17.5×10^6 (1.2×10^5)	Tin Bronze 16×10^6 (1.1×10^5)
Steel	30×10^6 (2×10^5)	2300 (191)	2180 (181)	2160 (179)	2100 (174)	1950 (162)	1900 (158)
Malleable iron	25×10^6 (1.7×10^5)	2180 (181)	2090 (174)	2070 (172)	2020 (168)	1900 (158)	1850 (154)
Nodular iron	24×10^6 (1.7×10^5)	2160 (179)	2070 (172)	2050 (170)	2000 (166)	1880 (156)	1830 (152)
Cast iron	22×10^6 (1.5×10^5)	2100 (174)	2020 (168)	2000 (166)	1960 (163)	1850 (154)	1800 (149)
Aluminum bronze	17.5×10^6 (1.2×10^5)	1950 (162)	1900 (158)	1880 (156)	1850 (154)	1750 (145)	1700 (141)
Tin bronze	16×10^6 (1.1×10^5)	1900 (158)	1850 (154)	1830 (152)	1800 (149)	1700 (141)	1650 (137)

Poisson's ratio = 0.30.

*When more exact values for modulus of elasticity are obtained from roller contact tests, they may be used.

Table 2.5 Elastic coefficient

2.6.10 AGMA strength equations

The equation for the allowable bending stress is:

$$\sigma_{all} = \frac{S_t}{S_F} \frac{Y_N}{K_R K_T} \quad [2.40]$$

Where

S_t : allowable bending stress

S_F : AGMA safety factor

Y_N : stress-cycle factor for bending stress

K_T : temperature factor

K_R : reliability factor

The equation for the allowable contact stress is

$$\sigma_{c,all} = \frac{S_c}{S_H} \frac{Z_N}{K_R K_T C_H} \quad [2.41]$$

Where

S_c : allowable contact stress

S_H : AGMA safety factor

Z_N : stress-cycle factor

C_H : hardness-ratio factor for pitting resistance

K_T : Y_θ temperature factor

K_R : reliability factor

So, what is the purpose of these two equations? Strength in gears is given empirically from charts. They are not related to other strengths such as S_{uth}, S_y or S_e and they should only be considered in gear design.

2.6.11 Hardness-Ratio factor, Z_W

The pinion is subjected to more cycles than the gear because it has smaller diameter. A uniform surface strength is obtained by making the surface of the pinion harder than the gear. The hardness-ratio factor is used only for the gear because it is overwhelmed more than the pinion. For pinion Z_W=1. For gear Z_W is obtained from the equation:

$$C_H = 1 + A'\left(m_G - 1\right) \qquad [2.42]$$

Where

$$A' = 8.98\left(10^{-3}\right)\frac{H_{BP}}{H_{BG}} - 8.29\left(10^{-3}\right)$$

$$1.2 < \frac{H_{BP}}{H_{BG}} < 1.7$$

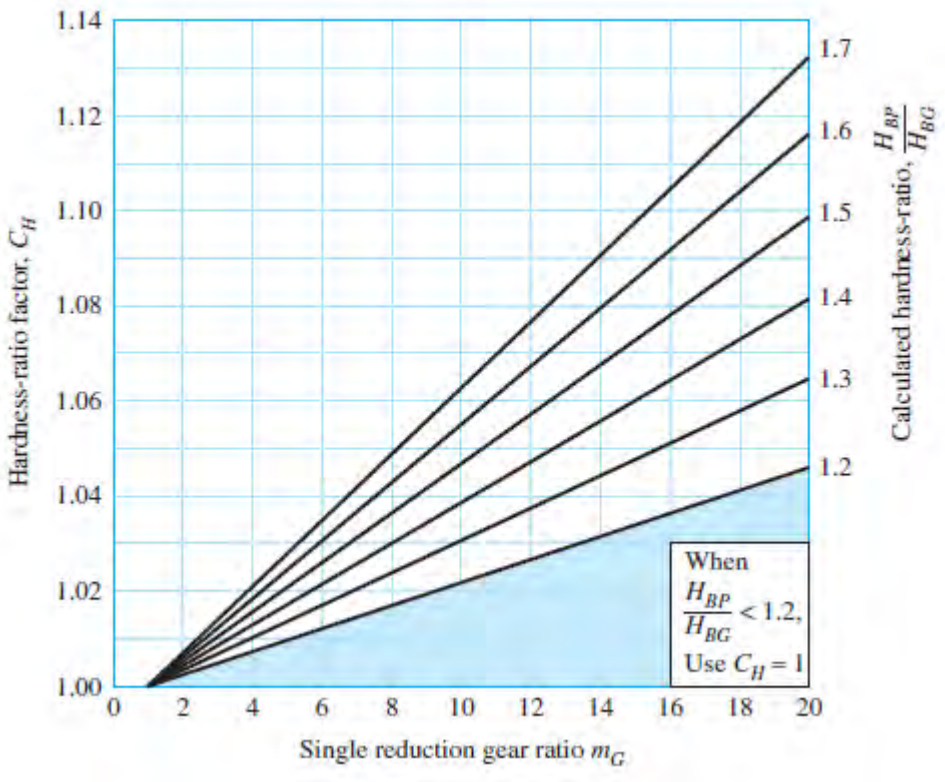

Figure 2.26 Hardness ratio factor

The terms H_{BP} and H_{BG} are the Brinell hardness (10-mm ball at 3000-kg load) of the pinion and gear, respectively.

2.6.12 Reliability factor, K_R

The reliability factor is a statistical measure that tells us the failures occurred on material fatigue tests. The values of Y_Z are given in the **Table 2.6** below:

Reliability	K_R (Y_Z)
0.9999	1.50
0.999	1.25
0.99	1.00
0.90	0.85
0.50	0.70

Table 2.6 Reliability factor

2.6.13 Temperature factor, K_T

The temperature factor for temperatures below 120 degrees Celsius is equal to 1. If the temperature is above 120 degrees Celsius the following equation is used:

$$\mathbf{K_T = \frac{238 + T}{327}} \qquad [2.43]$$

2.6.14 Stress-cycle factor Y_N

The repeatedly applied bending strength stress-cycle factor Y_N is given from **Figure 2.27**:

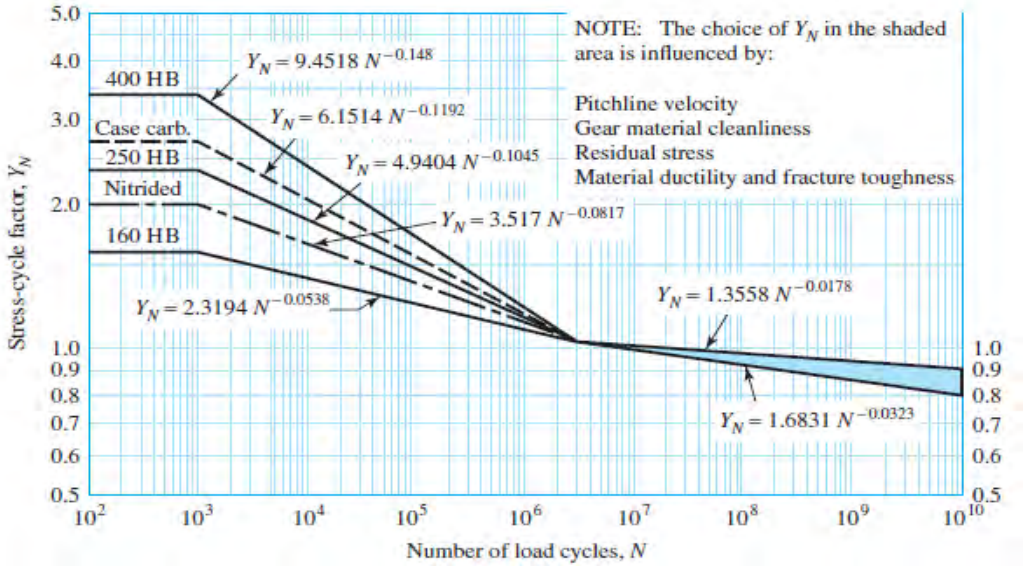

Figure 2.27 Stress-cycle factor for repeatedly bending strength

The pitting resistance stress-cycle factor Z_N is given from **Figure 2.28**.

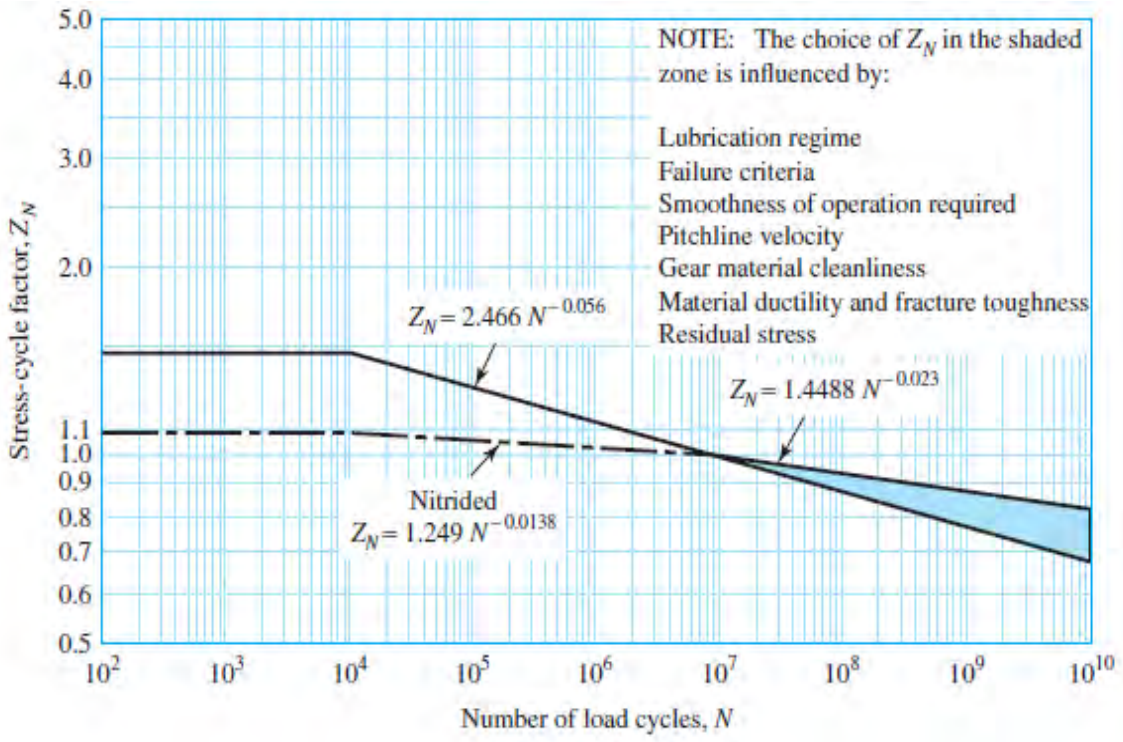

Figure 2.28 Stress-cycle factor for pitting resistance

2.6.15 Allowable Bending Stress, S_t

In order to determine the allowable bending stress, the hardness of the material needs to be known, then it is determined from the following figure:

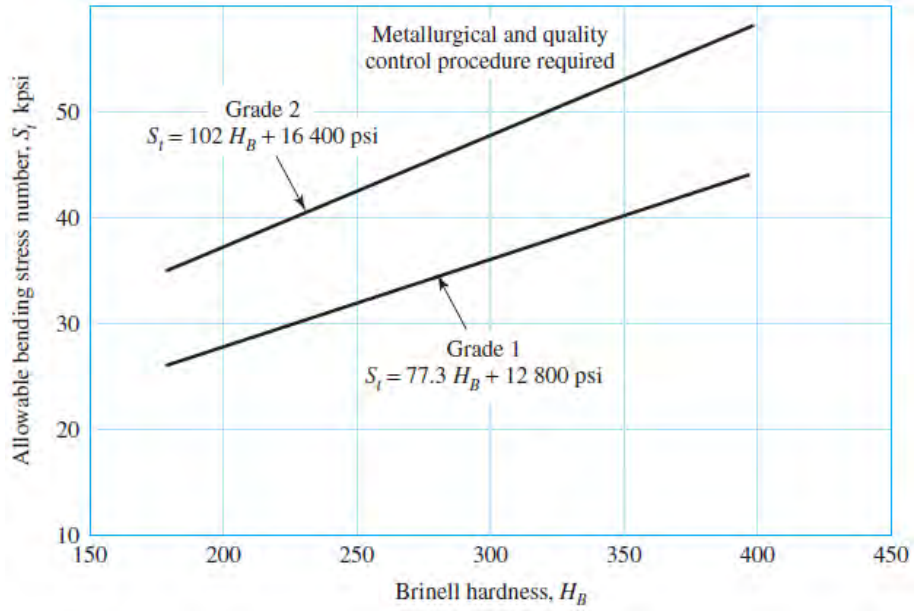

Figure 2.29 Allowable bending stress for Grade 1 and 2 (Brinell hardness)

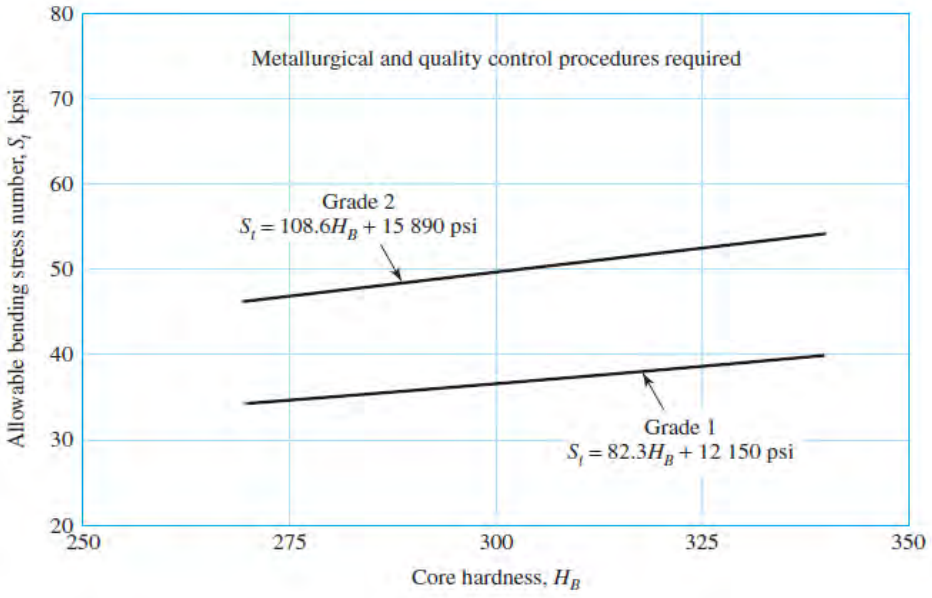

Figure 2.30 Allowable bending stress for Grade 1 and 2 (Core hardness)

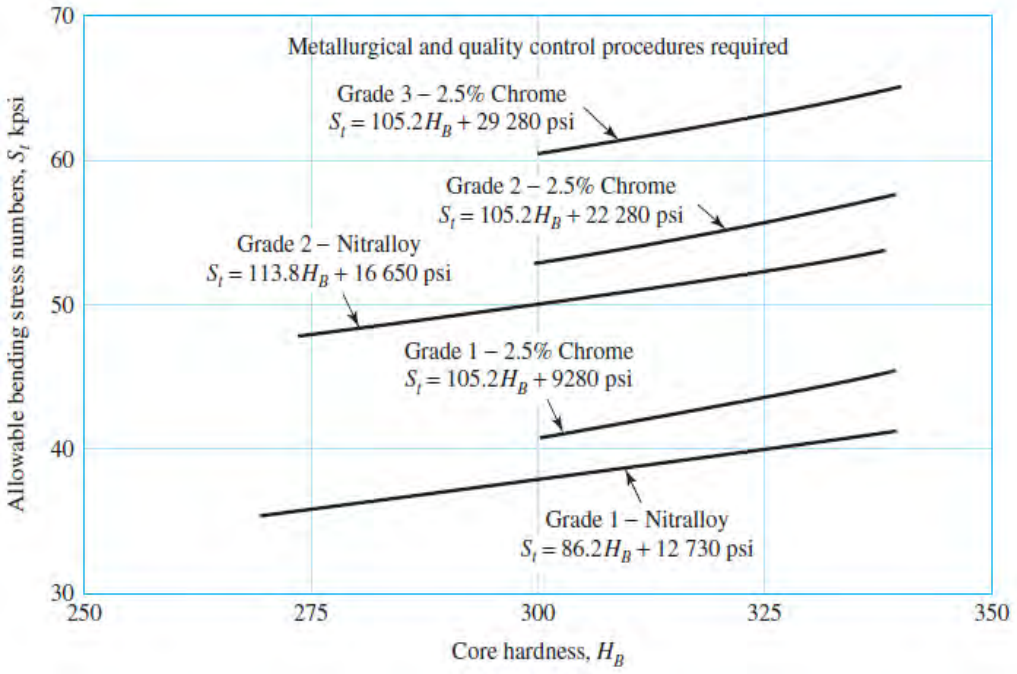

Figure 2.31 Allowable bending stress for various Grades (Core hardness)

2.6.16 Allowable Contact Stress, S_c

The allowable contact stress is given below [**Figure 2.32**]:

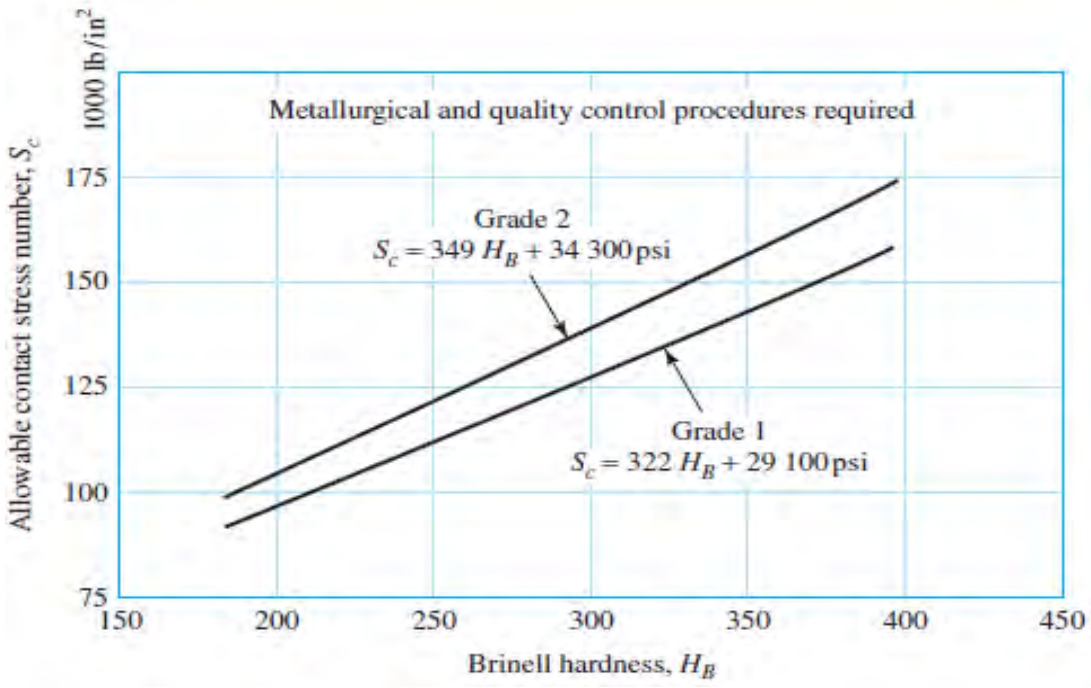

Figure 2.32 Allowable contact stress for Grade 1 and 2 (Brinell hardness)

2.6.17 Safety Factors S_F and S_H

The definition of safety factors is given from the equations below:

$$S_F = \frac{\sigma_{all}}{\sigma} \quad [2.44]$$

And

$$S_H = \frac{\sigma_{c,all}}{\sigma_c} \quad [2.45]$$

Further analysis about the safety factors is represented in chapter 5.

3 Spur Gear design & drawing

3.1 Case Study

A 22-tooth 20^o pressure angle spur pinion rotates at 1200 rpm and transmits 11.18 kW to a 60-tooth gear. The module is 4.23 mm, the face width is 50.8 mm and the quality standard is No. 8. The gears are straddle-mounted with bearings immediately adjustment. The material is alloy steel **31NiCr14** with Poisson's ratio of 0.3 and Young's modulus of 206 GPa. The pinion has a hardness of 240 Brinell tooth surface and through-hardened core and the gear has, also hardness of 200 Brinell tooth surface and core. The load is smooth because of motor and load. The tooth profile is uncrowned. The desired number of cycles is 10^8 and reliability is 0.9 This is a commercial enclosed gear unit.

3.2 AGMA results

In order to avoid or reduce errors caused by human interactions, an Excel file which contains all the AGMA factors and calculations has been created. The minimum input data required are: power (kW), pinion speed (rev/min), material selection (Young's modulus, Poisson's ratio), quality of gears, pinion life (cycles), reliability, module (mm), number of teeth, face width (mm). Hence, the initial input data, the secondary input data and the computed data are shown below. Another aspect of creating this excel, is that it can easily be applied in similar cases just by changing the initial inputs and the AGMA coefficients, depending on the problem.

	A	B	C	D
1	***Design Of Spur Gears***			Application
2				
3	**Initial Input Data:**			
4	Input Power:	P=	11185,50	Watt
5				
6	Input Speed:	n_p=	1200,00	rpm
7	Module:	m=	4,23	mm
8	Diametral Pitch:	P_d=	0,24	
9	Pressure angle:	ϕ=	20,00	deg
10	Number of Pinion Teeth:	N_P=	22,00	
11	Desired Output Speed:	n_G=		
12	Coputed number of gear teeth:			
13	Enter Chosen Number of Gear teeth:	N_G=	60,00	
14				
15	***Computed Data:***			
16	Actual output speed:	n_G=	440	rpm
17	Gear Ratio:	m_G=	2,727272727	
18	Pitch Diameter-Pinion	D_P=	93,126	mm
19	Pitch Diameter-Gear:	D_G=	253,98	mm
20	Center Distance:	C=	173,553	mm
21	Pitch Line Speed:	V=	5,851279149	m/s
22	**Transmitted Load:**	W_t=	1911,633288	N
23	Torque:	T=	89011,3808	N*mm
24				
25	**Secondary Input Data:**	Min	Nom	Max
26	Face width Guidelines (mm):	33,864	50,8	67,728
27	Base radius pinion, r_P=	43,754908		
28	Base radius Gear, r_G=	119,33157		
29	Poisson ratio pinion, v_P=	0,3		
30	Poisson ratio pinion, v_G=	0,3		
31	Young's Modulus pinion, E_P=	206000	[MPa]	
32	Young's Modulus pinion, E_G=	206000	[MPa]	
33	Desired Number of Cycles, N=	100000000	[cycles]	

Figure 3.1 Basic gear parameters, with grey color the characteristics that are introduced manually are highlighted

The Excel displays two main results. Firstly, all the stress parameters which comprise the transmitted load, torque, dynamic factor, geometry factor etc. Then, the pinion and the gear parameters which contain the bending and pitting stresses and their corresponding factors of safety. The procedure used to calculate all the AGMA factors is described below.

Bending Stress for Pinion & Gear			Safety Factors Bending		
	$(\sigma)_P$=	94,5662 [MPa]		$(S_F)_P$=	3,42681
				$(S_F)_G$=	3,97142
	$(\sigma)_G$=	83,0684 [Mpa]			

Contact Stress for Pinion & Gear			Safety Factors Contact		
	$(\sigma_c)_P$=	478,6 [Mpa]		$(S_H)_P$=	1,28595
	$(\sigma_c)_G$=	480,158 [Mpa]		$(S_H)_G$=	1,31171

Note: Gray colour cell means these values are user enterd values.

Factors in Design Analysis:		
Overload Factor, K_o=	1	
Dynamic Effect Factor, K_V=	1,28216	
A=	70,7222	
B=	0,62996	
Transmission accuracy level, Q_v=	8	
Maximum Pitch line velocity, $(V)_{max}$	28,6693	m/s
Size Factor, K_s		
$(K_s)_P$=	1,09129	
$(K_s)_G$=	1,0984	
Lewis Form Factor		
Y_P=	0,331	
Y_G=	0,422	
Load Distribution Factor, K_m=	1,32219	
C_{mc}=	1	
C_e=	1	
C_{pm}=	1	
C_{pf}=	0,04207	
C_{ma}=	0,28012	
Rim-Thickness Factor, K_B=	1,38	
Bending Strength geometry factor		
$(Y_J)_P$=	0,24	
$(Y_J)_G$=	0,275	

Hertzian Stress σ_c

Factors in Design Analysis:	
C_P=	189,812
Speed ratio, m_G=	2,72727
I=	0,11758
Surface condition factor, C_f=	1

Figure 3.2 AGMA coefficients calculation sheet

Allowable Bending Stress			Allowable Contact Stress		
$(\sigma_{all})_P$=	324,5429	[MPa]	$(\sigma_{c,all})_P$=	912,519	[MPa]
$(\sigma_{all})_G$=	330,3909	[MPa]	$(\sigma_{c,all})_G$=	933,8211	[MPa]
Stress number, S_t=	282,42	[MPa]	Pitting resistance stress cycle		
Reliability factor, K_R=	0,85		$(Z_N)_P$=	0,948437	
Temperature factor, K_T=	1		$(Z_N)_G$=	0,970577	
Hardness ratio factor, C_H=	1		Contact Stress Number, S_c=	817,81	[MPa]
Stress Cycle factor:					
$(Y_N)_P$=	0,976777				
$(Y_N)_G$=	0,994378				

Figure 3.3 Allowable stresses computational sheets

In the final part of the excel file the allowable stresses are calculated in order to define the safety factors that was represented in **Figure 3.2**.

3.2.1 Calculation of computed data

The calculations that are automatically done from the excel are analytically represented below:

Gear ratio:

$$m_G = \frac{N_G}{N_P} = \frac{60}{22} = 2.73$$

Where N_P, N_G are the teeth number of pinion and gear respectively.

Actual output speed:

$$n_G = \frac{n_P}{m_G} = \frac{1200}{2.727} = 440 \text{ [rpm]}$$

Where n_P is the pinion input speed in rounds per minute.

Pitch diameter pinion:

$$D_P = mN_P = 93.13 \text{ [mm]}$$

Where m is the module of pinion and gear.

Pitch diameter gear:

$$D_G = mN_G = 253.98 \text{ [mm]}$$

Center distance:

$$C = \frac{(D_P + D_G)}{2} = 173.55 \text{ [mm]}$$

Pitch line speed:

$$V = \frac{\pi D_P n_P}{60000} = 5,85 \text{ [m/s]}$$

Transmitted load:

$$W^t = \frac{P}{V} = 1911,63 \text{ [N]}$$

Where P is the input power.

Torque:

$$T = \frac{W^t D_P}{2} = 89011,38 \text{ [N mm]}$$

3.2.2 Calculation of Bending stress

The bending stresses for pinion and gear are given by equation [**2.28].**

$$\sigma_b = \frac{W^t K_o K_V K_m K_s K_B}{mFY_j}$$

Assuming uniform loading, according to table **Table 2.3** overload factor, K_o, is set as one. To evaluate, K_V, from equation **[2.30]** with a quality number Q_V=8, firstly parameters A and B are calculated.

$$B = \frac{(12 - Q_V)^{2/3}}{4} = 0,63$$

$$A = 50 + 56(1 - B) = 70,72$$

The dynamic factor is evaluated as shown below

$$K_V = \left(\frac{A + \sqrt{200V}}{A}\right)^B = 1,28$$

To determine the size factor from equation **[2.33]** the face width (F), module and Lewis form factor are needed. From table **[2.2]** for N_P=22 (number of pinion teeth) Lewis form factor takes the value Y_P=0.331 while gear for N_G=60, Y_G=0.422.

$$(K_S)_P = 1.192(0.0394^2 Fm\sqrt{Y_P})^{0.0535} = 1,09$$

$$(K_S)_G = 1.192(0.0394^2 Fm\sqrt{Y_G})^{0.0535} = 1,1$$

The size factor equation is in SI units where face width and module are in millimeters.

The load distribution factor is determined from equation [**2.34],** where five terms are needed to be evaluated.

For uncrowned teeth K_{mc}=1.

For straddle-mounted pinion with $S_1/S<0.175$, $K_{pm}=1$

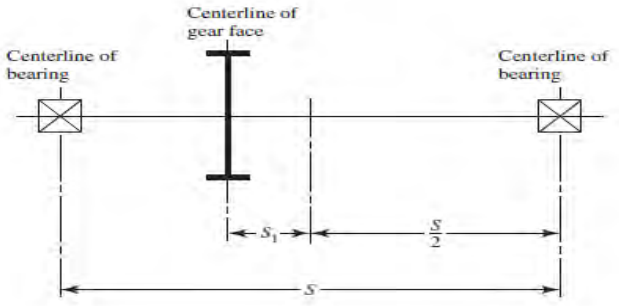

Figure 3.4 Load distribution factor parameters definition depending on the position of the gear considering the bearings

For face width F=50.8 mm

$$K_{pf} = \frac{F}{10d_P} - 0.0375 + 0{,}0004925F = 0{,}04$$

C_e=1 as shown in the figure below

$$C_e = \begin{cases} 0.8 & \text{for gearing adjusted at assembly, or compatibility is improved by lapping, or both} \\ 1 & \text{for all other conditions} \end{cases}$$

Figure 3.5 C_e constant value determination depending on the adjustment of the gears assembly

Last term is C_{ma} where is calculated from equation $\boldsymbol{C_{ma} = A + BF + CF^2}$ where values of A, B and C are taken from **Table 2.4**.

$$\boldsymbol{C_{ma} = A + BF + CF^2 = 0{,}28}$$

The load distribution factor can be evaluated as shown below

$$K_m = K_{mf} + K_{mc}(K_{pf}\, K_{pm} + C_{ma}C_e) = 1{,}32$$

The rim-thickness factor is evaluated from the final form of the geometry of pinion and gear respectively as it is going to be presented in the next chapter. To evaluate this factor **Figure 2.24** is used and the value is K_B=1.38.

The last bending stress factor is the geometry factor of pinion and gear which can be evaluated from the diagram in **Figure 2.25**

$$(Y_j)_p = 0.24$$

$$(Y_j)_G = 0.28$$

The bending stress for pinion and gear can be calculated substituting the appropriate terms as shown below.

$$(\sigma_b)_P = \frac{W^t K_o K_V K_m (K_s)_P K_B}{mF(Y_j)_P} = 94,57 \text{ [MPa]}$$

$$(\sigma_b)_G = \frac{W^t K_o K_V K_m (K_s)_G K_B}{mF(Y_j)_G} = 83,07 \text{ [MPa]}$$

3.2.3 Calculation of contact stress

The evaluation of contact stress can be done from the following equation

$$\sigma_C = Z_E \sqrt{\frac{W^t K_o K_V K_S K_m Z_R}{FD_P Z_I}}$$

There are three terms in this equation that have to be evaluated, Z_E, Z_R and Z_I.

Assuming that there is no defect on the surfaces of pinion and gear, that can cause a non-uniformity on the contact stresses, surface condition factor is set as C_f=1.

From equation **[2.38],** surface strength geometry factor is evaluated as shown below

$$Z_I = \frac{\cos\varphi \sin\varphi}{2} \frac{m_G}{m_G + 1} = 0,12$$

Where m_G is the Gear ratio.

The elastic coefficient, Z_E, can be estimated from the equation **[2.39]** as shown

$$Z_E = \sqrt{\frac{1}{\pi\left(\frac{1-\nu_P^{\,2}}{E_P} + \frac{1-\nu_G^{\,2}}{E_G}\right)}} = 189,81$$

Where ν_P, ν_G are the Poisson's ratio and E_P, E_G are the Young's modulus of pinion and gear respectively.

The bending stress for pinion and gear can be calculated substituting the appropriate terms as shown below.

$$(\sigma_C)_P = Z_E\sqrt{\frac{W^t K_o K_V (K_S)_P K_m Z_R}{F D_P Z_I}} = 478,62 \text{ [MPa]}$$

$$(\sigma_C)_G = Z_E\sqrt{\frac{W^t K_o K_V (K_S)_G K_m Z_R}{F D_P Z_I}} = 480,17 \text{ [MPa]}$$

3.2.4 Allowable bending stress

The allowable bending stress takes place as it has to calculate a value that will set the upper limit to the bending stress of the design.

$$\sigma_{all} = \frac{S_t Y_N}{K_R K_T}$$

From table **[2.4]** with reliability of 0.9 the reliability factor resulting K_R=1. It is assumed that the oil temperature is below 120 degrees Celsius so the temperature coefficient K_T=1.
In order to estimate the stress number S_t, from **Figure 2.29** with a Brinell hardness of 240 [MPa] for pinion and 200 [MPa] for gear, the value is estimated to be S_t=282.42 [MPa].
The last term is the stress cycle factor which is calculated for pinion and gear separately. The AGMA strengths as given for life of 10^8 cycles give the stress cycle factor from the equation.

$$(Y_N)_P = 1.3558N^{-0.0178} = 0,98$$

$$(Y_N)_G = \frac{(Y_N)_P}{m_G^{-0.0178}} = 0,99$$

The allowable bending stress for pinion and gear can be calculated substituting the appropriate terms as shown below.

$$(\sigma_{all})_P = \frac{S_t (Y_N)_P}{K_R K_T} = 324,54 \text{ [MPa]}$$

$$(\sigma_{all})_G = \frac{S_t (Y_N)_G}{K_R K_T} = 330,39 \text{ [MPa]}$$

3.2.5 Allowable contact stress

The allowable contact stress takes place as it has to calculate a value that will set the upper limit to the contact stress of the design.

$$\sigma_{C_{all}} = \frac{Z_N S_C}{K_R K_T C_H}$$

The hardness ratio factor is set as C_H=1 because the hardness ratio H_{Bp}/ H_{BG}<1.2. (**Figure 2.26**).
The pitting resistance stress cycle factor which is calculated for pinion and gear separately is calculated from **Figure 2.28** from equation

$$(Z_N)_P = 1.4488 N^{-0.023} = 0,95$$

$$(Z_N)_P = 1.4488 N^{-0.023} = 0,97$$

The last term, Contact stress number S_C, is evaluated from the equation of the **Figure 2.32** and takes the value of S_C=817.81 [MPa]

The pitting resistance allowable bending stress for pinion and gear can be calculated substituting the appropriate terms as shown below.

$$(\sigma_{C_{all}})_P = \frac{(Z_N)_P S_C}{K_R K_T C_H} = 912,52 \text{ [MPa]}$$

$$(\sigma_{C_{all}})_G = \frac{(Z_N)_G S_C}{K_R K_T C_H} = 933,82 \text{ [MPa]}$$

3.2.6 Safety factors

The AGMA standards contain a safety factor S_F against bending fatigue failure and a safety factor S_H against pitting resistance. The evaluation takes place below.

Safety factor for pinion and gear against bending stress:

$$(S_F)_P = \frac{(\sigma_b)_P}{(\sigma_{all})_P} = 3,43$$

$$(S_F)_G = \frac{(\sigma_b)_G}{(\sigma_{all})_G} = 3,98$$

Safety factor for pinion and gear against contact stress:

$$(S_H)_P = \frac{(\sigma_c)_P}{(\sigma_{Call})_P} = 1,91$$

$$(S_H)_G = \frac{(\sigma_c)_G}{(\sigma_{Call})_G} = 1,95$$

For the pinion, a comparison between $(S_F)_P$ and $(S_H)_P{}^2$ is made, or 3.43 with 1.906^2 = 3,64, so the threat in the pinion is from bending. For the gear, comparing $(S_F)_G$ with $(S_H)_G{}^2$, or $3,977065$ with $1,944755^2$= 3,782072010025 so the threat in the gear is from wear.

3.3 Spur gear drawing in Solidworks (CAD)

3.3.1 Modeling parameters

In order to properly draw the pinion and the gear an Excel file has been created, which concludes all the necessary parameters for design. The minimum input data required are: module (mm), number of pinion teeth, number of gear teeth. All the calculations were made in Excel and the results are shown below.

Pinion			**Gear**	
Module (m):	4		Module (m):	4.23
Number of teeth (N_p):	22		Number of teeth (N_g):	60
Pressure angle (ϕ):	20		Pressure angle (ϕ):	20
Diameter (d_p):	93.06		Diameter (d_g):	253.8
Circular pitch (p_c) :	13.289		Circular pitch (p_c) :	13.289
Diametral pitch (P):	0.2364		Diametral pitch (P):	0.2364
Addendum (a):	4.23		Addendum (a):	4.23
Dedendum(b) :	5.2875		Dedendum(b) :	5.2875
Clearance (c):	1.0575		Clearance (c):	1.0575
Addendum diameter (d_a)	101.52		Addendum diameter (d_a)	262.26
Dedendum/root diameter (d_r)	82.485		Dedendum/root diameter (d_r)	243.23
Total depth (h_t):	9.5175		Total depth (h_t):	9.5175
Working depth (h_k):	8.46		Working depth (h_k):	8.46
Radius of base circle (r_b)	43.724		Radius of base circle (r_b)	119.25
Base pitch (p_b):	12.488		Base pitch (p_b):	12.488

Figure 3.6 Basic gear characteristics essential for the drawing of the gear and pinion in SOLIDWORKS CAD

The significance of this file is the data extraction about the efficiency of the gearing. Factors like contact length, contact ratio, center distance, face width guidelines are shown below.

Pinion-Gear		
Contact length (L_{ab})	21,0128128	
Contact ratio (m_c)	1,68270558	
Tooth thickness (th)	6,644468462	
Backlash (b_l)	(table 3.1)	
Center Distance (C_d)	173,43	
Face width	33,84	67,68

Figure 3.7 Basic characteristics of gear and pinion

The backlash selection depends on the module and its value varies as it is represented in **Table 3.1** below:

Module *m*	Backlash, mm
1	0.05-0.10
2	0.08-0.13
3	0.10-0.15
4	0.13-0.20
5	0.15-0.23
6	0.18-0.28
8	0.23-0.36
10	0.28-0.41
12	0.35-0.51
18	0.46-0.69
25	0.63-1.02

Table 3.1 Backlash variation depending on the module

As it is computed, there will be no interference between the two mating gears, so counter actions like undercutting are not needed.

maximum possible addendum circle radius without interference		Addendum radius	Control
Pinion	73.69	50.76	No Interference
Gear	133.2	131.13	No Interference
the smallest number of teeth on the pinion without interferenc	16	No Interference	

Figure 3.8 Determination of the possible interference between gear and pinion during the meshing

3.3.2 Spur gear and pinion drawing

Under the following steps an equation driven spur gear can be modeled in Solidworks (CAD).

Step 1: In order to properly model the spur gear "Equations" are used as shown below.

Equations, Global Variables, and Dimensions

Filter All Fields

Name	Value / Equation	Evaluates to	Comments
Global Variables			
"m"	= 4.233mm	4.233mm	Module
"Np"	= 22	22	Number of Pinion Teeth
"phi"	= 20deg	20deg	Pressure angle
"Dp"	= "m" * "Np"	93.126	Pitch diameter
"Da"	= "Dp" + 2 * "m"	101.592mm	Addendum diameter
"Dd"	= "Dp" - 2 * 1.25 * "m"	82.5435mm	Dedendum diameter
"Db"	= "Dp" * cos ("phi")	87.5098deg	Base diameter

Figure 3.9 Parametric equations

Step 2: The addendum circle is sketched and extruded to get the pinion body.

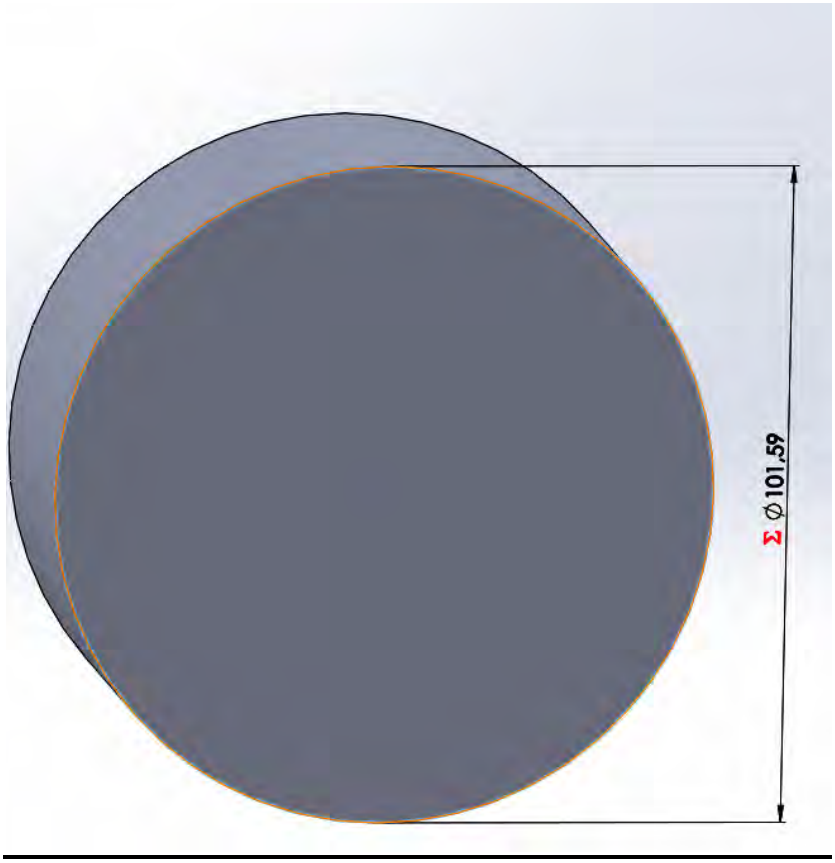

Figure 3.10 Addendum circle extrude

Step 3: Pitch circle, Base circle and Dedendum circle are drawn at the surface of the pinion body.

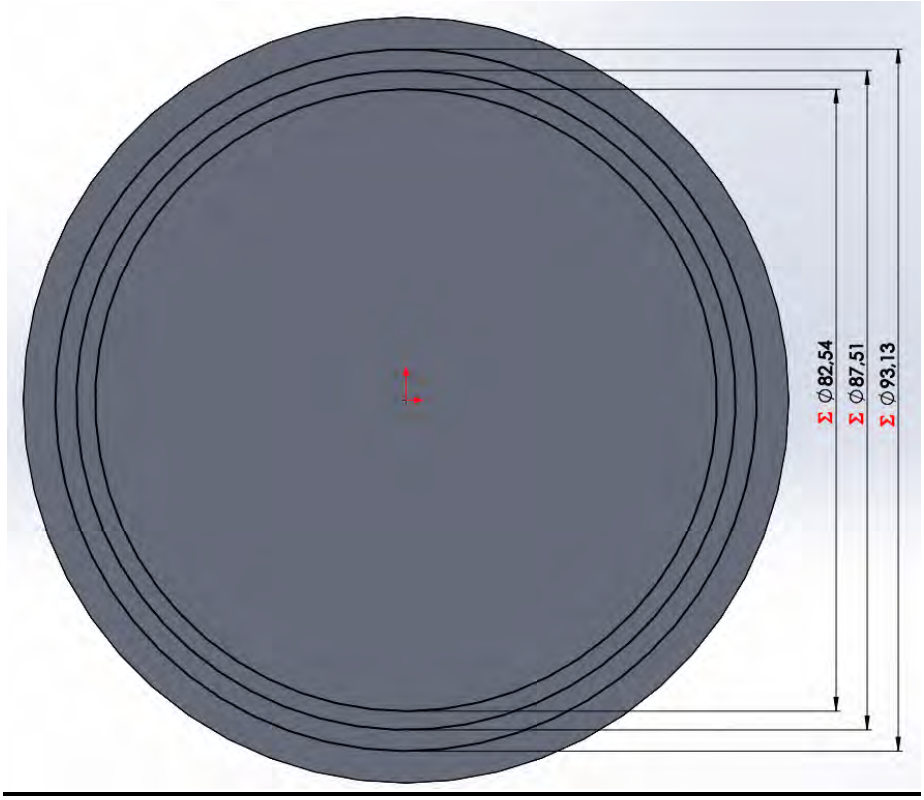

Figure 3.11 Characteristic circles extracted from the parametric equations

Step 4: The involute tooth profile is created under the same sketch.

The parametric equations of the involute curve are:

$$x = r\cos t + rt\sin t = r(\cos t + t\sin t)$$

$$y = r\sin t - rt\cos t = r(\sin t - t\cos t)$$

The involute curve starts from point A. Note that the involute starts from the base circle.

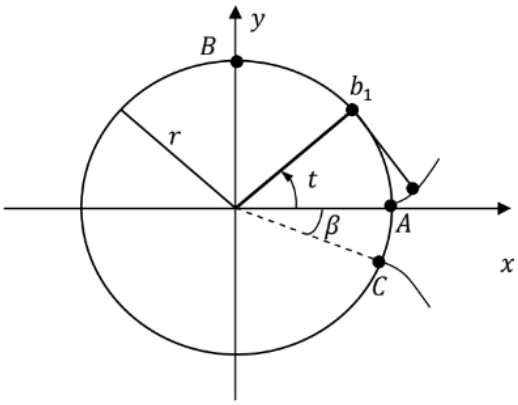

Figure 3.12 Involute curve generation theory

Since the number of teeth is known, the angle corresponds to the circular pitch can be defined.

$$\frac{360^\circ}{N_P} = \frac{360^\circ}{22} = 16.363636...^\circ$$

Since tooth thickness is the same as width of space, there are four equally distributed angles along the circular pitch.

$$\frac{360^\circ}{4N_P} = 4.09090909...^\circ$$

As illustrated in the following diagram, α can be defined as

$$\alpha = \frac{\sqrt{d_p{}^2 - d_b{}^2}}{d_b} - \varphi = 0.014904384°$$

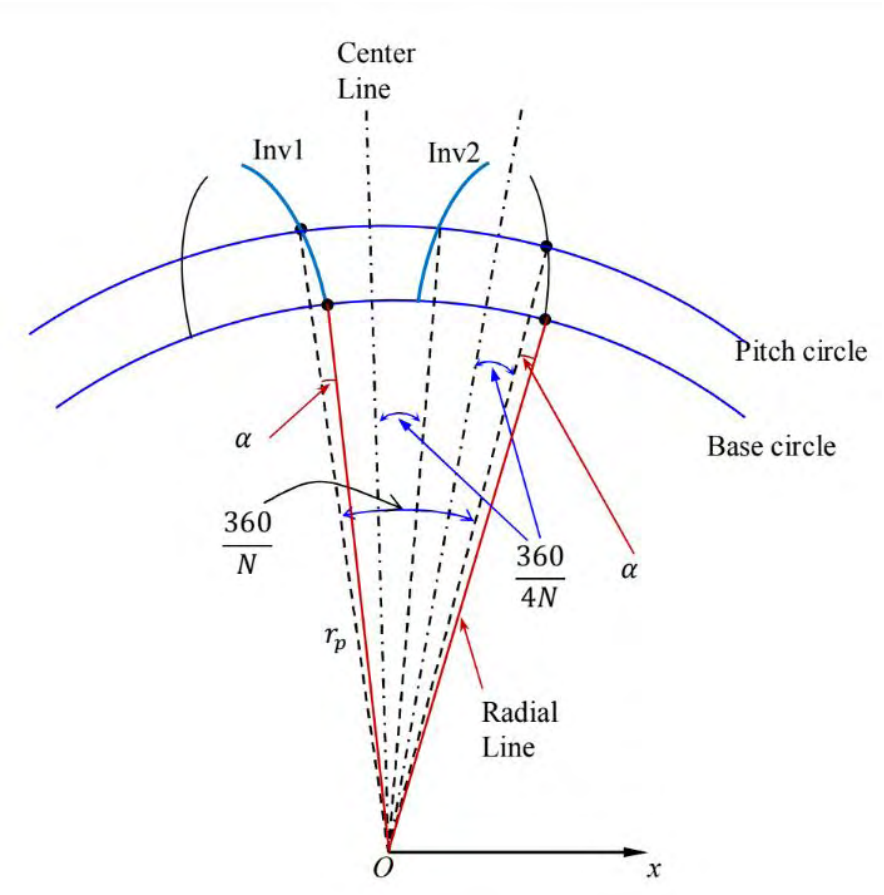

Figure 3.13 Basic angle geometrical illustration

The expression for creating the involute tooth profile in Solidworks CAD: (Tools → Sketch entities → Equation Driven Curve).

$$X(t) = "D2@Sketch2"*0.5*(\cos(t) + t*\sin(t))$$

$$Y(t) = "D2@Sketch2"*0.5*(\sin(t) - t*\cos(t))$$

Note that "D2@Sketch2" is the dimension of the base circle diameter.

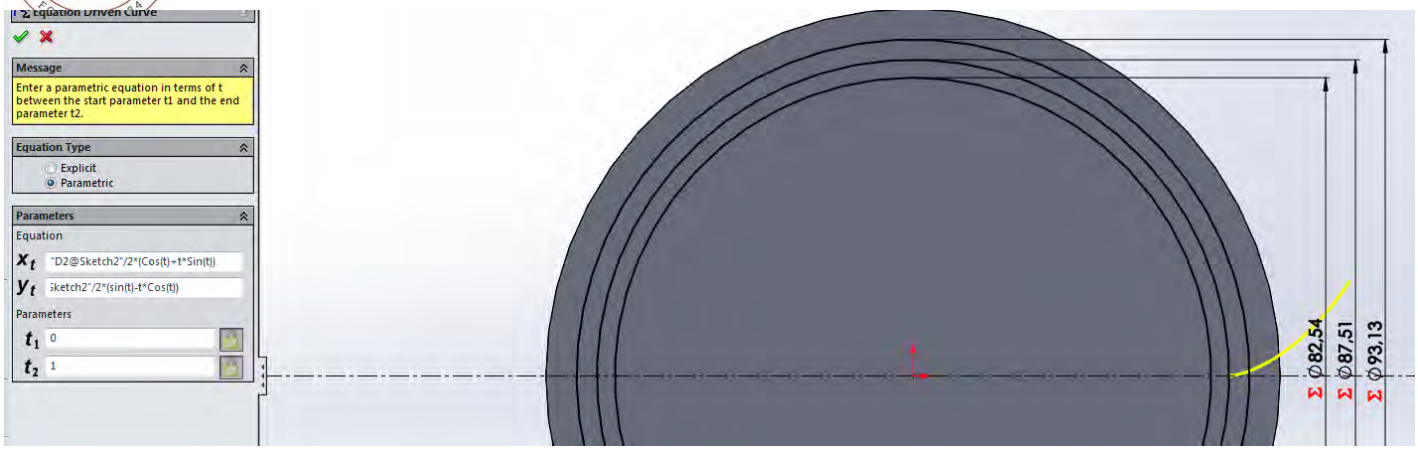

Figure 3.14 Involute generation in SOLIDWORKS

Step 5: After mirroring the involute profile at $\frac{360°}{4N_P} = 4.09090909...°$ and using the "Extrude cut" the width of space is created.

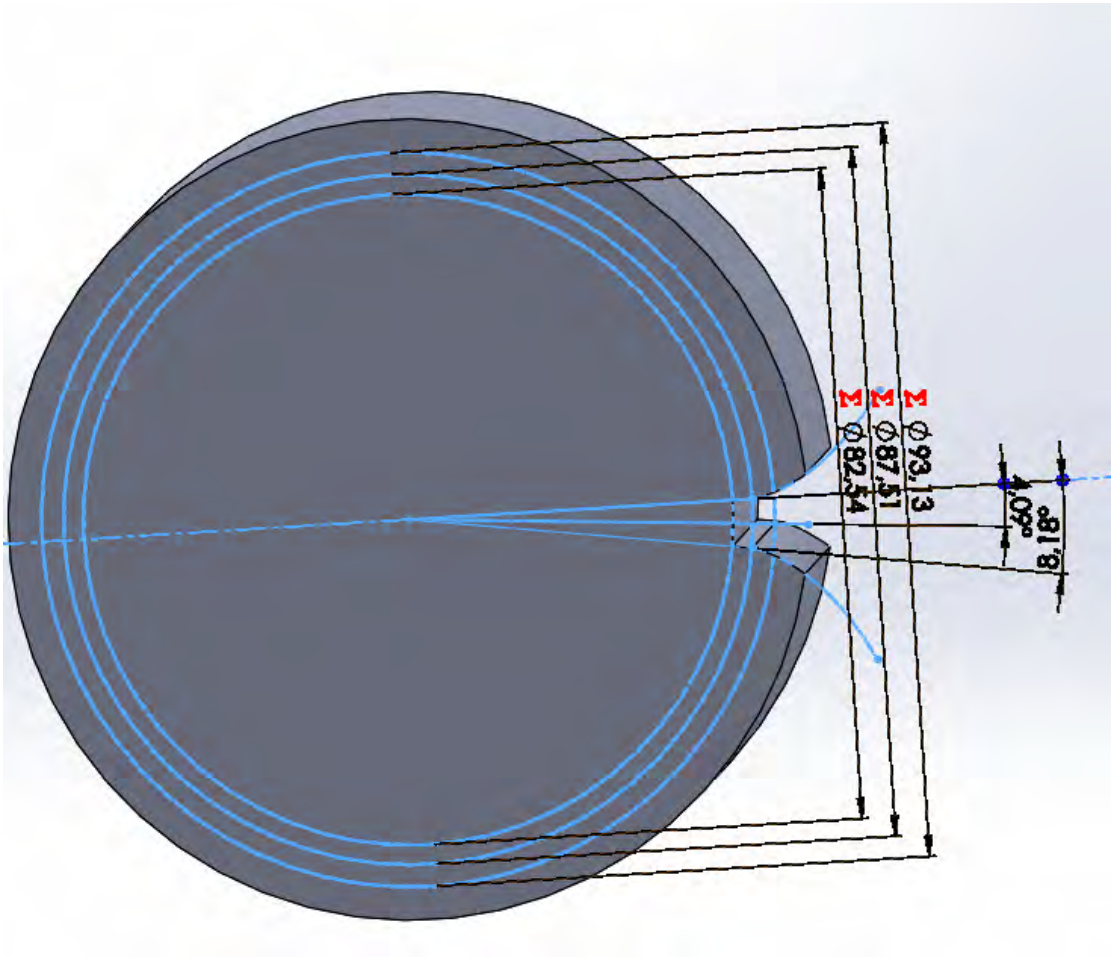

Figure 3.15 Involute curve mirroring and cut extrude

Step 6: The number of width of spaces is equal to the number of the pinion teeth, so after the "fillet" creation, circular pattern follows which results to the final form of the pinion.

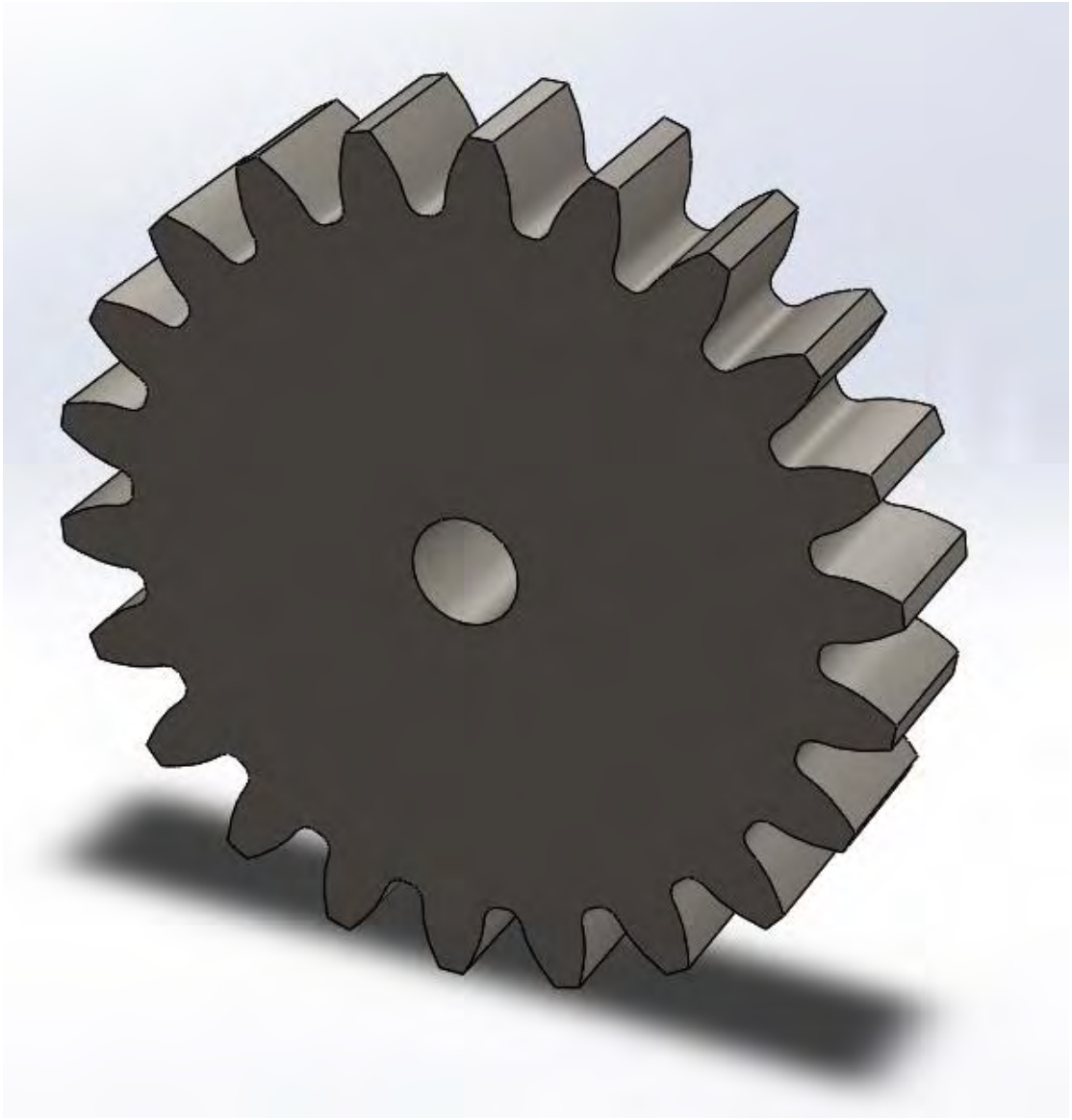

Figure 3.16 Pinion SOLIDWORKS model

Following the same strategy Gear is also modeled. The result is shown in the next figure.

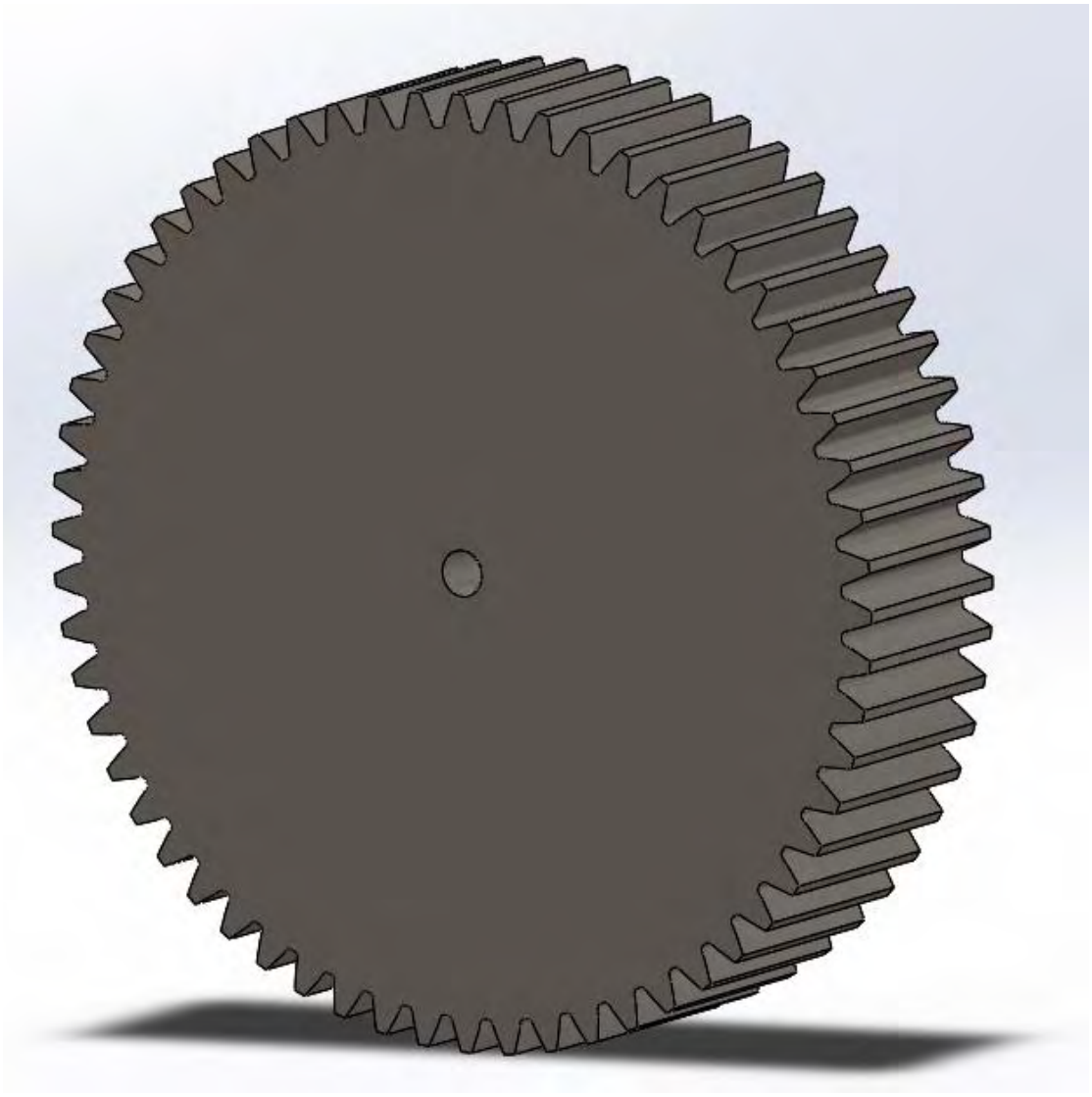

Figure 3.17 Gear SOLIDWORKS model

3.3.3 Assembly

The assembly of the two parts consists of the following mates.

- The front faces of the pinion and the gear are set to be coincident with the Front plane.
- The axes of rotation of both pinion and gear are set to be coincident with the Top plane.
- The axis of rotation of pinion are set to be coincident with the Right plane

- Both axes of rotation have a mating distance between then about $C_d = \frac{d_P + d_G}{2}$
- Both axes of rotation have a mechanical “gear” mate with gear ratio of

The result is shown in the following figure.

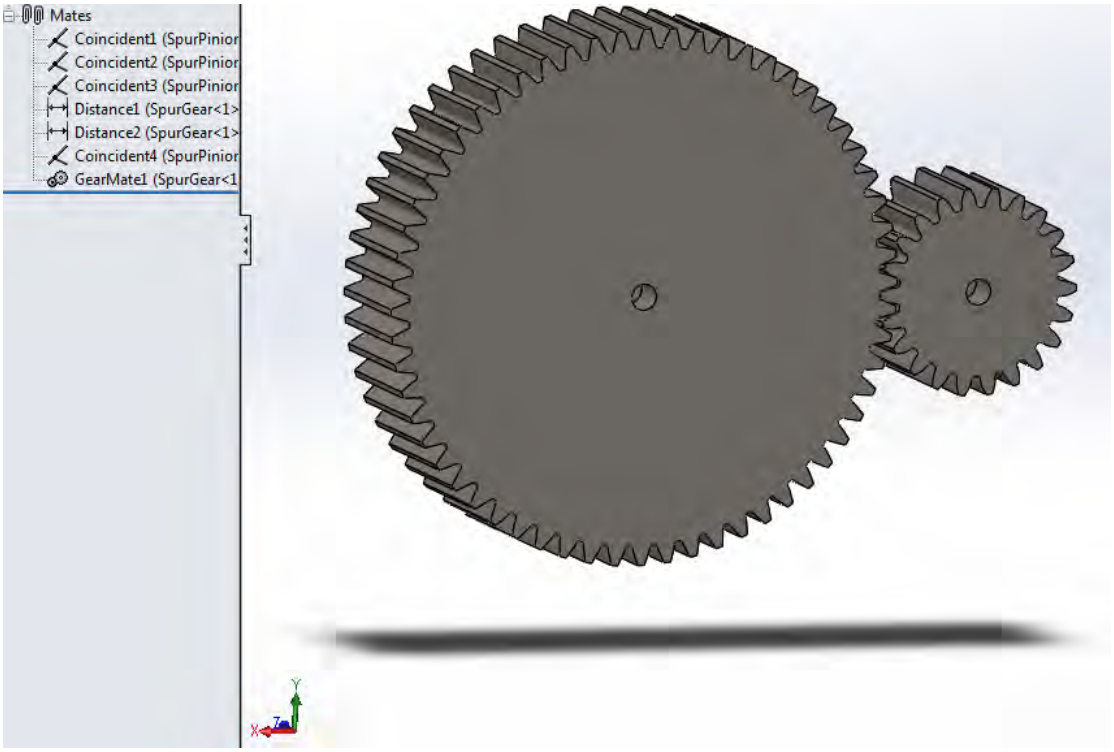

Figure 3.18 Completed gear-pinion assembly

3.3.4 Simplified geometry for Finite Element Analysis

Gear engagement results in deployment of stresses at the surface and at the root of teeth. This means that a large part of the gear does not need to be examined. In order to avoid making a model with too many elements it is decided to cut off the "useless" geometry part from pinion and gear. This will result in less process time and will make the model lighter. The final form of the geometry is presented below.

Figure 3.19 Final assembly geometry

The final part is to extract a 2-D face, as the finite element analysis will be two dimensional, for the reason that for spur gears there is no geometry change in the third axis so the results of the 2-D analysis are sufficient.

4 FE Modelling (ABAQUS)-Preparation of the model

The finite element method, is a numerical method solving partial differential equations (PDE) and is commonly used for engineering problems. First of all, the PDE expressing the physical phenomenon of our problem must be defined. Next, by integrating, the weak form of our problem is extracted, while the PDE form is considered the strong one. The following step is the discretization of the weak form, where the integral is converted to a summation, in order to be solved numerically. The main intention in discretization is to transform the integral form in a set of matrixes so the problem can be approached with known matrixes algebra.

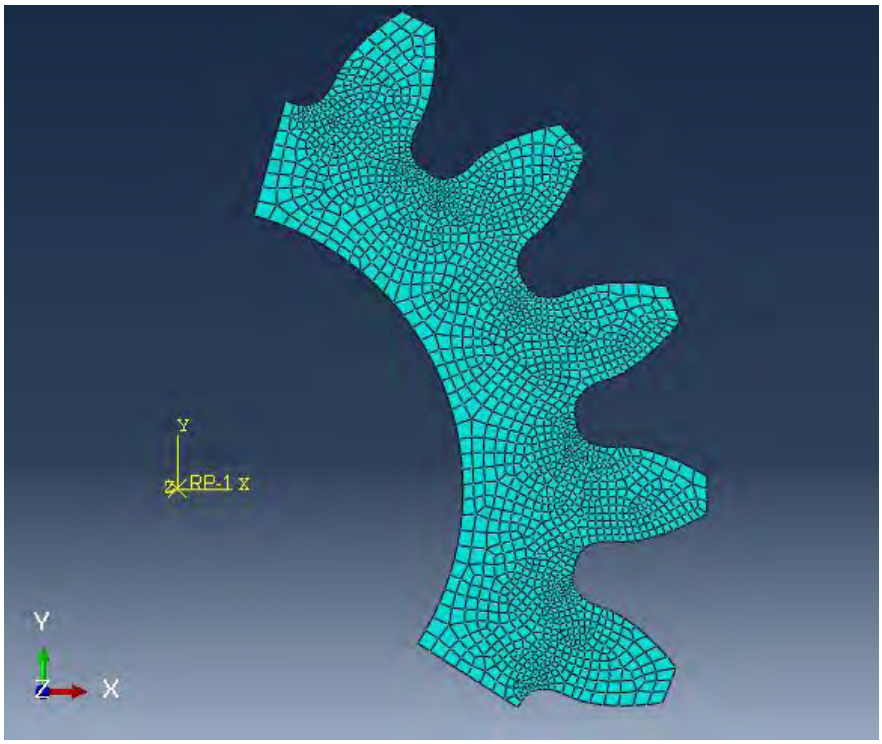

Figure 4.1 Pinion with a not refined mesh

As shown in **Figure 4.1** the part is divided in smaller and simpler pieces called "elements" and each element consists of nodes in a certain position of its body,

depending on the element type and family. The calculation of the characteristic function is applied on the nodal point and interpolation is used for the whole element. In this particular thesis the mathematical part of finite element method is not going to be analyzed.

4.1 Abaqus model initiation

Having exported a parasolid file of the gear and pinion assembly from SOLIDWORKS, first thing that needs to be done is the importation of the geometry in the ABAQUS CAE interface. By right-clicking on Parts on the model tree and selecting Import, the assembly geometry is added in the part module of ABAQUS.

4.2 Material definition

Afterwards, the material properties of the gear and pinion must be defined. The chosen material is an alloy structural steel 31NiCr14 heat treaded with mechanical and chemical properties as seen in the following tables:

C	Si	Mn	Ni	S	P	Cr	Cu
0.27-0.33	0.17-0.37	0.3-0.6	2.75-3.15	Max:0.025	Max:0.025	0.6-0.9	Max:0.3

Table 4.1 Chemical properties of selected alloy

Density(kg/m^3)	Tensile Strength(Mpa)	Yield Stress(Mpa)	Young Modulus(Gpa)	Poisson Ratio
7870	980	785	206	0.3

Table 4.2 Mechanical properties of selected alloy

In the following analysis it is assumed that the pinion and the gear have only elastic behavior for the reason that the yield stress is equal to 785 Mpa while the maximum stresses occurred in the gears engagement are reaching up to 630 Mpa, according to the AGMA standard analysis. More details about the results will be given in the next chapter. For the material definition in the ABAQUS, the elastic coefficients that are introduced are Young Modulus and Poisson's Ratio and Density, equal to the ones in the **Table 4.2** and they are assigned to each one of the gear and pinion. The assembly of the two instances is made in SOLIDWORKS, so the following part is creating the interactions of the analysis.

4.3 Interaction properties

It is critical that the contact interaction between the gear and the pinion is made with caution and that it is correct, as it has a powerful impact on the results of the finite element analysis. The selected interaction is the surface to surface pair algorithm. The reason is that the contacting faces between the gear and the pinion are known, so the master and slave surfaces can be chosen manually, while avoiding unnecessary computational load which comes with the general contact algorithm. Firstly, the pinion is selected as the master surface and the gear as the slave as in **Figure 4.2**, where with red color is highlighted the possible master contact surfaces and with pink the possible slave surfaces They both consist of the same material, so the reason for that selection is that the pinion's hardness is higher than the gear's one and specifically, as shown in **3.1**, pinion has hardness of **240 Brinell** while the gear **200 Brinell.**

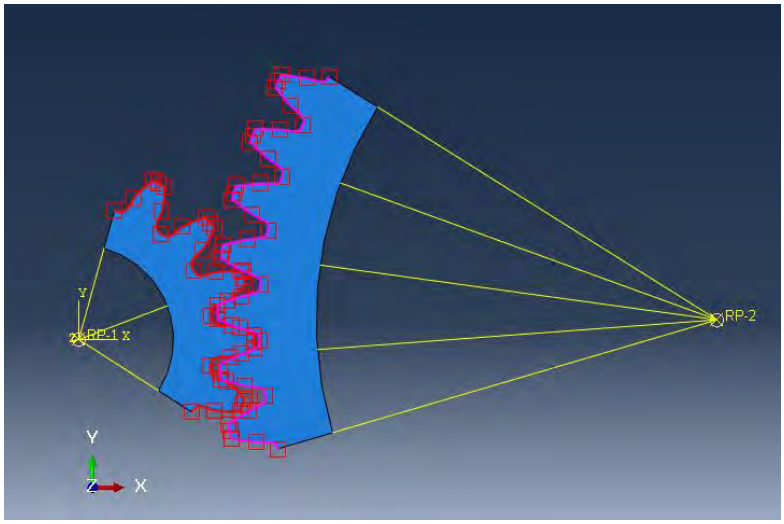

Figure 4.2 Surface to surface contact-Master and slave surfaces selection

As for the discretization method surface to surface method is preferred instead of node to surface discretization. Using this method, the shape of both master and slave faces are taken in consideration, so the contact conditions are applied in a region surrounding the slave nodes and not in just an individual slave node (node to surface), as a result no considerable undetected penetration of master nodes in some slave ones is happening. Generally, comparing the two methods, the surface to surface is providing more accurate and reliable results concerning the contact stresses that occurring during the gear meshing.

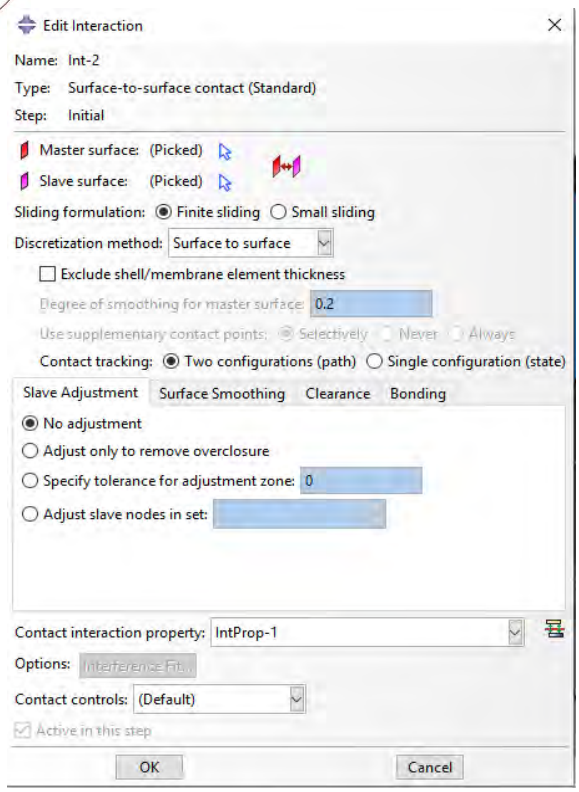

Figure 4.3 Defining contact interaction

For the node tracking of the opposing contacting bodies, the finite sliding approach is being used as it allows for arbitrary separation, sliding, and rotation of the surfaces.

Next thing that needs to be defined is the interaction property and for this particular case the contact property. Specifically, tangential and normal behavior are determined, where friction is chosen with a coefficient equal to 0.05 as it is assumed that the gears are lubricated, additionally in the normal behavior field hard contact seems to be the most appropriate one for this case as it allows pressure transmission through the contacting faces. With hard contact bodies remain detached until clearance is less than or equal to zero, also contact continues as long as the transmitted pressure is less than zero.

In order to reduce computational cost, the shaft is not included in the model, thus it is crucial that a way to simulate it is found, and that is accomplished through the coupling constraint. Coupling constraints, are used to constraint the motion of a surface to that of one or more reference points. In this particular model, the inner surfaces of the gears are attached to their centers, as in **Figure 4.2** and all degrees of freedom are constrained with a kinematic coupling type.

4.4 Analysis Steps-Boundaries and load conditions

The problem is divided in the three following steps:

First comes the **contact step**, where the initiation of the contact takes place. In the beginning of the analysis the two components are considered to be detached so with load application, while the system is in isolation, convergence is improbable. There are two escape routes for this obstacle. One is using contact stabilization; however, this method is chosen when connection is unclear and the clearance between the contacting surfaces is unknown, thus the contact initiation is achieved with a rotation of the pinion by a significantly small angle, while the gear is fixed (constrained in all degrees of freedom). By creating a displacement rotation boundary condition for the pinion in the contact step, internal stresses are developing, however they are not in line with the external loading so in the following step, the **load step**, the pinion is reset to its original position by rotating it backwards with the inversed displacement. Simultaneously, the gear is set free to rotate and the design torque multiplied by the gear ratio is applied on it as a moment load. The final step is the **rotation step**, where the pinion is rotating by a single contact cycle opposing the revolution of the gear resulting from the moment load. A better view of the analysis steps is represented in the table below:

Steps	Pinion		Gear	
	Moment Load (T)	Rotation(R3)	Moment Load (T)	Rotation (R3)
Contact	0	r_c	0	0
Load	0	$-r_c$	T_d	Free
Rotation	0	r_p	T_d	Free

Table 4.3 Analysis steps

Where $\mathbf{r_c}$ is the rotation angle of the pinion and is equal to **0.0009 radians**, or **0.05 degrees**. The design torque that is transmitted from the shaft to the pinion is equal to **89 (N*m)**, so the moment load that is introduced to the gear is $\mathbf{T_d}$**=242.727 (N*m)**. In the rotation step, $\mathbf{r_p}$ equals to **0.35 radians** or **20 degrees**, and it consist of one complete contact cycle, so the desired outputs can be extracted.

4.5 Mesh Selection

The final step before solving the problem is applying the mesh on the model. In order to select the proper mesh, some tests need to be done for selecting the appropriate number of elements, as the output results are mesh depended.

Attempt 1

Firstly, a default ABAQUS mesh was selected. The global seeds parameters are as seen in **Figure 4.4** below :

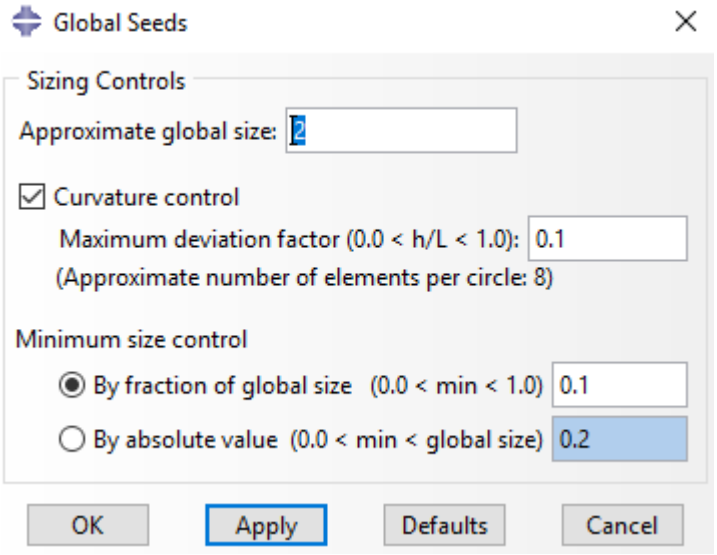

Figure 4.4 Global seeds parameters specification

Next one is the selection of the element shape from the mesh controls module:

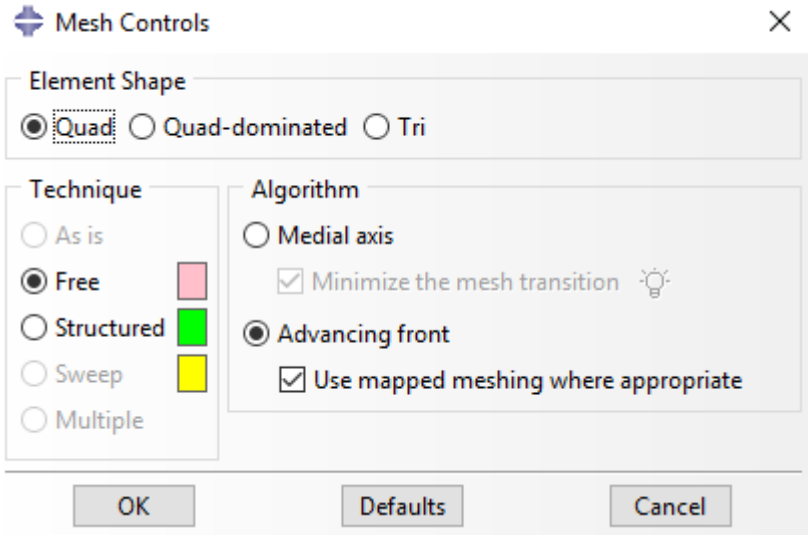

Figure 4.5 Mesh controls: Element shape selection

The element type that is chosen, is the CPS4R elements, which are 4-node bilinear plane stress quadrilateral reduced integration elements. The reason this type is selected is the nature of our problem, which is a contact problem and those elements provides us reliable results. In the following figure the element type parameters selection is represented:

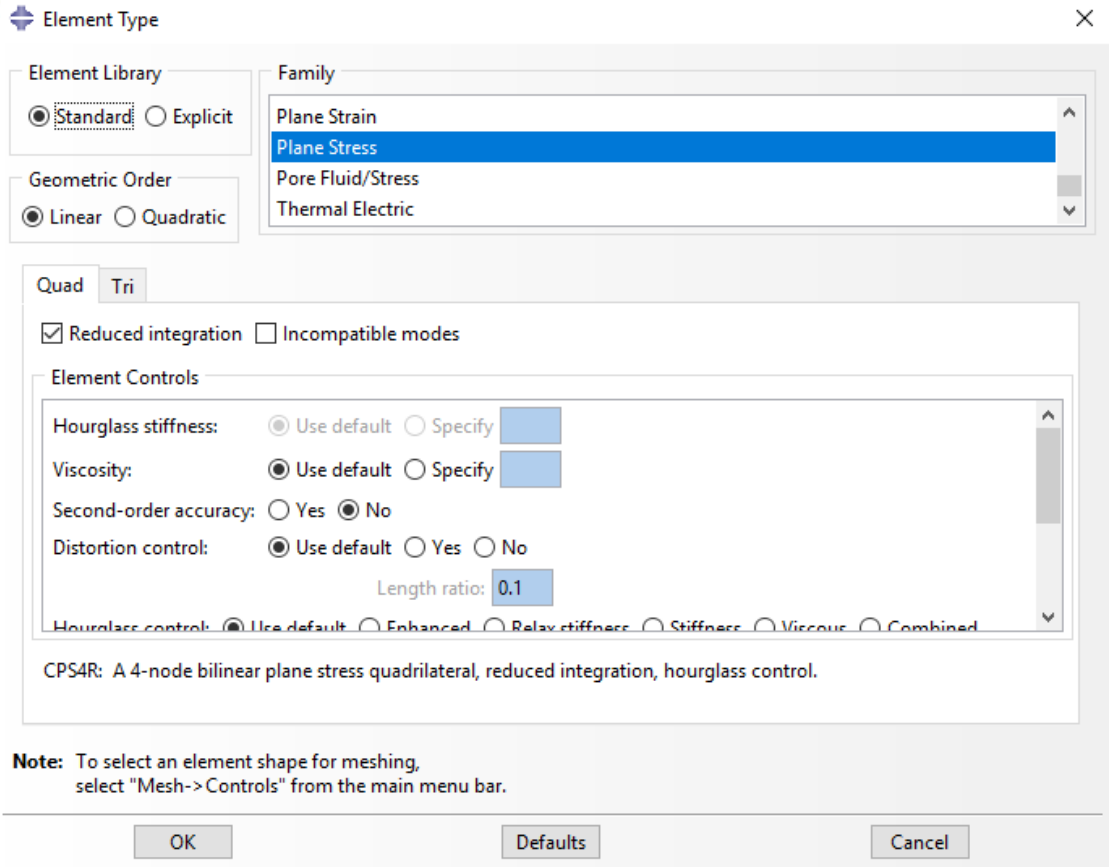

Figure 4.6 Element type selection

Afterwards, the mesh is generated, also it can be verified, but this particular mesh is not suitable for dealing with the problem. After submitting the model to the solver, the solution is extracted:

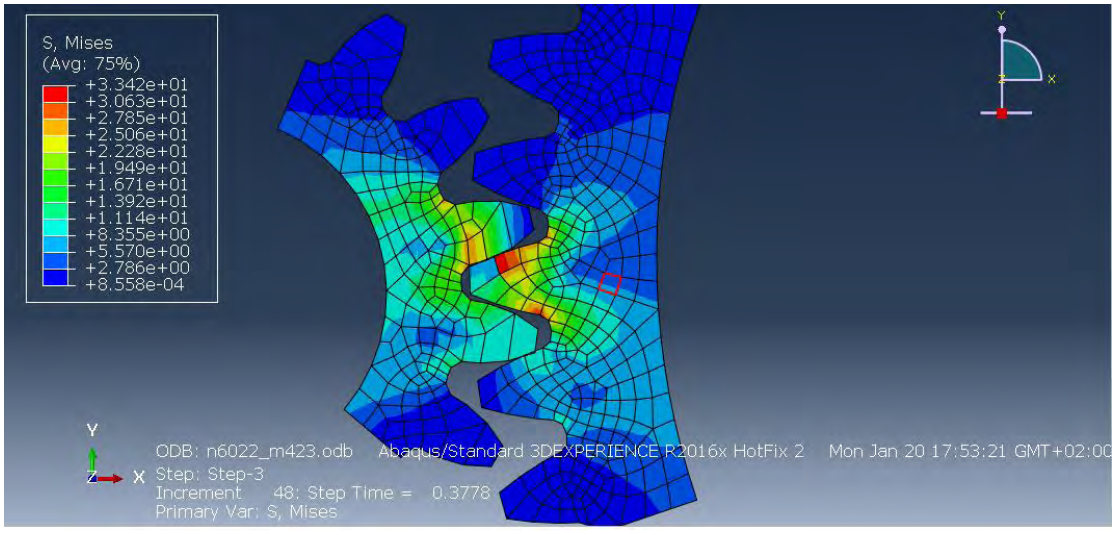

Figure 4.7 Attempt 1 : Von Mises stress distribution

The number of elements used for the pinion are 181 and for the gear are 417 so 598 in total for the entire model.

As it is shown in **Figure 4.7**, the maximum **Contact Stress** is **33.42 MPa** while the maximum **Bending Stress** is **29.12 MPa**. Those stresses abstain from the real ones and it is logical because of the coarse mesh selection. In order to conclude to a finer mesh some more attempts need to be tested.

Attempt 2

In the second attempt, local seed are used in the contact faces so the number of elements are increased topically in areas of interest. The areas of interest are the possible contacting faces as it is shown below.

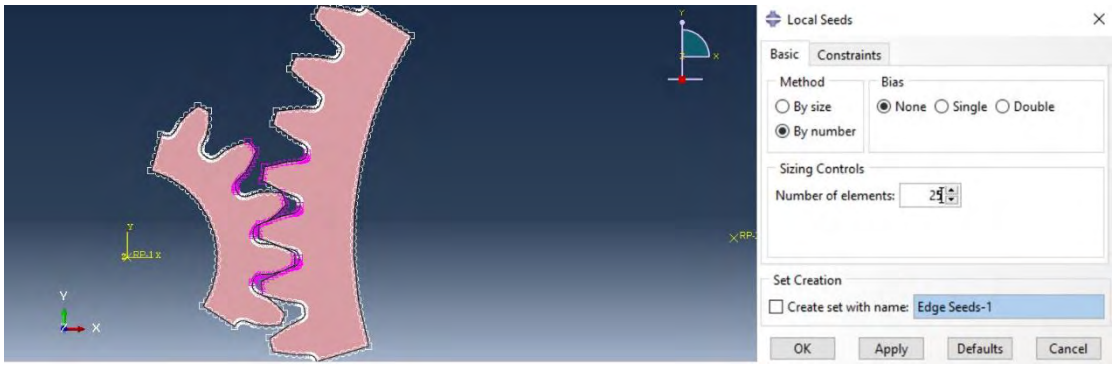

Figure 4.8 (a) Local seeds applied on surfaces of interest(pink), (b) Number of elements for each local seed surface

By doing this,the addition of pointless computational cost is avoided, while getting the valid results. Additionally, the approximate size of global seeds drops to 1 and the maximum deviation factor for the curvature control is chosen 0.02. By reducing the deviation factor the seeds are concentrating in the roots of the teeth, where the bending stress is located. By submitting the new model, the extracted results are the following:

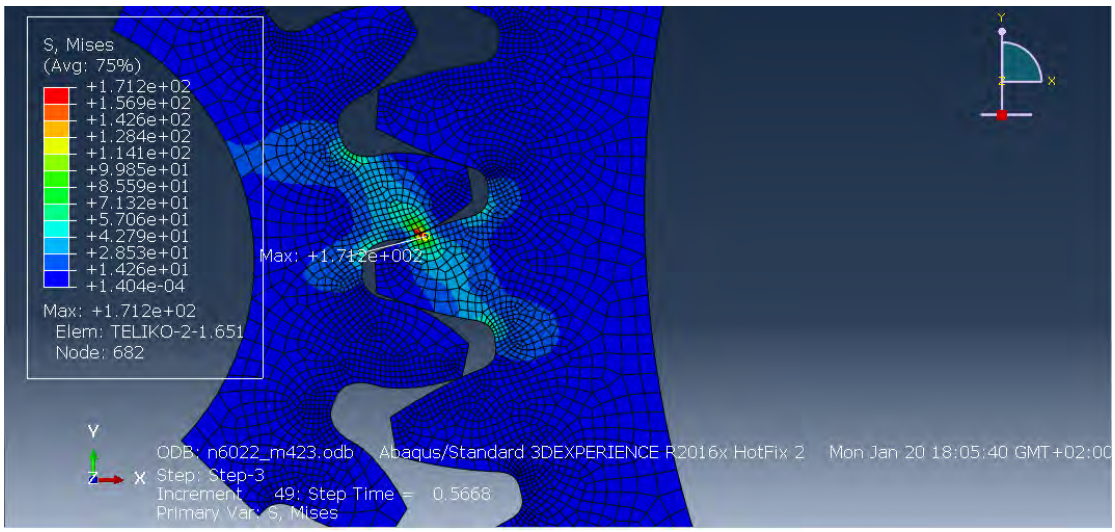

Figure 4.9 Attempt 2: Von Mises stress distribution

The number of elements used for the pinion are 1790 and for the gear are 2847 so 4637 in total for the entire model.

The maximum **Contact stress** for this attempt is **171.20 MPa** while the maximum **Bending** is **68.72 MPa**. A significant rise of the stresses magnitudes is observed; therefore, a denser mesh is needed so valid results can be obtained. In the following analyses the number of the local seeds are increasing and the deviation factor is decreasing so the change of the Contact and Bending stresses can be observed. The obtained results are represented in **Table 4.4** below:

Attempts	1	2	3	4	5	6	7	8
Global seeds-approximate size	2	1	0.8	0.5	0.5	0.5	0.5	0.5
Maximum deviation factor	0.1	0.02	0.02	0.01	0.01	0.01	0.003	0.003
Number of Local Seeds	-	25	40	100	300	370	390	410
Total Number of Elements	598	4637	8875	21950	61543	80113	84564	186462
Maximum Contact Stress (Mpa)	33.42	171.20	181.74	295.93	441.23	452.94	466.53	474.44
Maximum Bending Stress (Mpa)	29.12	68.72	79.25	80.64	79.15	80.12	83.14	87.11

Table 4.4 Maximum stresses variation, depending on mesh change

There is no need for further increase of elements, as there is no significant divergence in the maximum stresses. So the chosen model is the last one, with the larger number of elements:

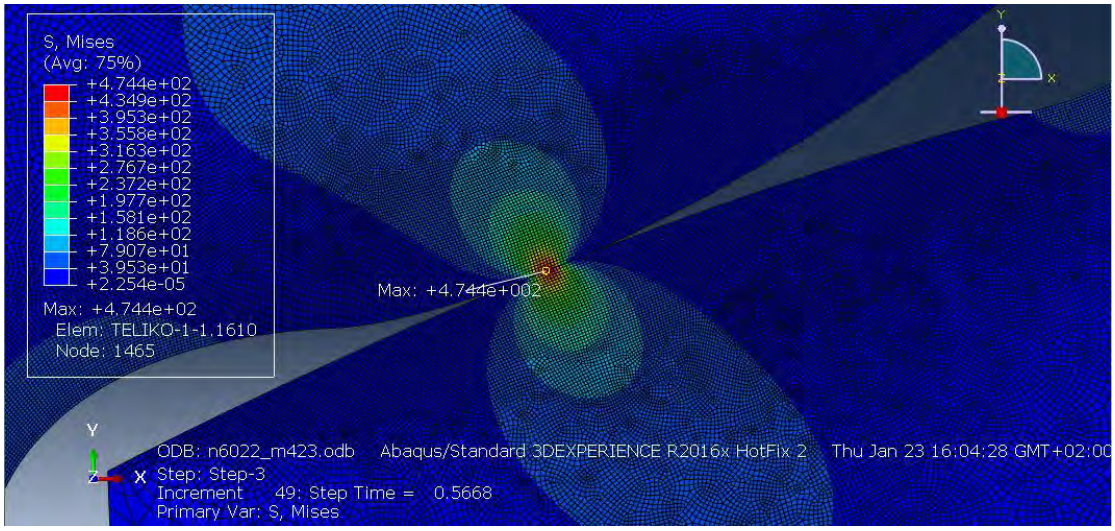

Figure 4.10 Maximum contact stress

Supplementary analysis regarding the results of the model, as well as comparison between them and those from the AGMA standard, is being shown in the following chapter.

5 FEA Results and AGMA standard comparison

The original goal of this thesis was to verify the AGMA standard contact and bending stress outputs by using the finite elements method. For a certain case study that is described in a previous chapter, the AGMA standard was applied and by creating an excel file using the spur gear geometry and AGMA equations from **Chapter 2 Spur Gear Basics**, various outputs were provided. The **Contact** and **Bending** stresses were considered as the main results in the analysis.

5.1 Bending Stress Comparison

In finite element analysis 8 models with progressive increase of element's numbers are examined. In the following **Diagram 5.1**, the iteration of FEA bending stress appearing on the pinion, is represented, where with yellow color is the **AGMA pinion bending stress** equal to **94.57 MPa**, while with orange color is shown the variation of **FEA bending stress**, which converges to the value of **87.11 MPa.**

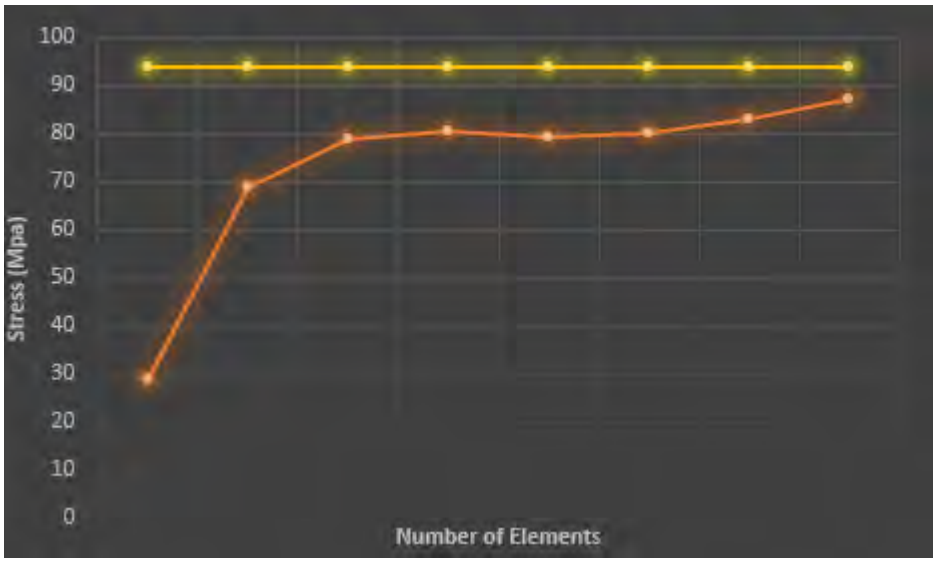

Diagram 5.1 Pinion bending stress alteration, considering the increase of the number of elements

Regarding the **gear bending stress**, the stress numbers obtained are smaller. This is a logical phenomenon as the gear is larger than the pinion so for the similar bending load, lower stresses are appearing. Explicitly, the **AGMA gear bending stress** is

$\boldsymbol{\sigma_G = 83.07\ (MPa)}$, while the result from ABAQUS is:

$\boldsymbol{\sigma_{GA} = 82.65 (MPa).}$

In both gear and pinion, the maximum bending stresses are the compressive ones taking place in the upper tooth root in the pinion, while in the gear in the lower tooth root. In ***Figure 5.1*** the maximum bending stress location on the lower half of the meshing gear tooth, is shown by hiding the pinion section in ABAQUS visualization module.

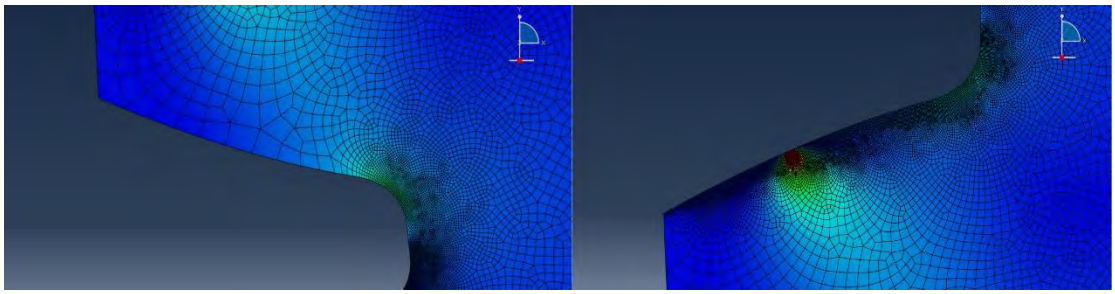

Figure 5.1 (a) Gear Compressive Bending Stress(maximum) , (b) Gear Contact Stress and Tensile Bending Stress

The elements mesh is denser in the areas that the maximum stresses are occurring so valid results are extracted. In the rest of the model the element size is bigger, in order to avoid pointless computational load.

5.1.1 Errors between AGMA and FEA

Considering the AGMA analysis as the correct method for gear designing, error can be computed from the finite element method results.

	Pinion	Gear
$\sigma_{bending}$(AGMA)	94.57 MPa	83.71 MPa
$\sigma_{bending}$(FEA)	87.11 MPa	82.65 MPa
Error	**7.9 %**	**1.2 %**

Table 5.1 Error from finite element analyzing for bending stress of pinion and gear

Hence, designing with AGMA a stricter limitation is applied on bending stresses. These high values result from considering that the bending load is applied on the tip of the tooth (**Figure 2.25**), therefore the worst case scenario is being inspected. Nevertheless, the two designing methods are close so the AGMA criterion is verified, as well the analyzing finite element method is valid.

5.1.2 Safety Factors

Safety factors was originally used in mechanical designs, to encounter uncertainties in the design analysis, in material characteristics and in manufacturing tolerances. As well as, human error risks and economic consequences of failure are taken in consideration. The greater the impact of those, the higher value is chosen for the safety factors. Better knowledge of the problem helps in selecting safety factor with satisfactory accuracy.
From AGMA standard by using the bending strength of the material:

$\boldsymbol{S_t = 282.42}$ $(\boldsymbol{MPa})$, a maximum allowable bending stress is extracted, and it is equal to: $\boldsymbol{\sigma_{allG} = 330.39}$ $(\boldsymbol{MPa})$, for the gear and $\boldsymbol{\sigma_{allP} = 324.54}$ $(\boldsymbol{MPa})$, for the pinion. Those numbers are by far greater than both bending stresses of the pinion and gear, as well as the ones provided by the FEA analysis. In the following ***Table 5.2***, the safety factors from AGMA and finite element analysis are shown.

	AGMA		Finite Element Analysis	
	Pinion	Gear	Pinion	Gear
Safety Factors	**3.43**	**3.98**	**3.73**	**3.99**

Table 5.2 Bending Stress safety factors for AGMA and FE analysis

Generally, the safety factors are defined from the designer depending on the application and the reliability of the materials that are used. A variety of characteristic values for safety factors is represented in the figure below.

Equipment	Factor of Safety - *FOS* -
Aircraft components	1.5 - 2.5
Boilers	3.5 - 6
Bolts	8.5
Cast-iron wheels	20
Engine components	6 - 8
Heavy duty shafting	10 - 12
Lifting equipment - hooks ..	8 - 9
Pressure vessels	3.5 - 6
Turbine components - static	6 - 8
Turbine components - rotating	2 - 3
Spring, large heavy-duty	4.5
Structural steel work in buildings	4 - 6
Structural steel work in bridges	5 - 7
Wire ropes	8 - 9

Applications	Factor of Safety - *FOS* -
For use with highly reliable materials where loading and environmental conditions are not severe and where weight is an important consideration	1.3 - 1.5
For use with reliable materials where loading and environmental conditions are not severe	1.5 - 2
For use with ordinary materials where loading and environmental conditions are not severe	2 - 2.5
For use with less tried and for brittle materials where loading and environmental conditions are not severe	2.5 - 3
For use with materials where properties are not reliable and where loading and environmental conditions are not severe, or where reliable materials are used under difficult and environmental conditions	3 - 4

Figure 5.2 Safety factor variation depending on the (a) Equipment that the materials are being used and (b) the properties and the reliability of the material that is used.

So depending on the condition of the problem the safety factor can be changed and as a result the tolerances of the design.

5.2 Contact stress comparison

The stresses appearing during the contact engagement are undoubtedly higher than the ones occurring in the root of the teeth, so extra caution should be given. In the following **Figure 5.3**, the change in stress magnitude on the gear contact stress from the finite element model, depending from the increase of the elements numbers, is being shown.

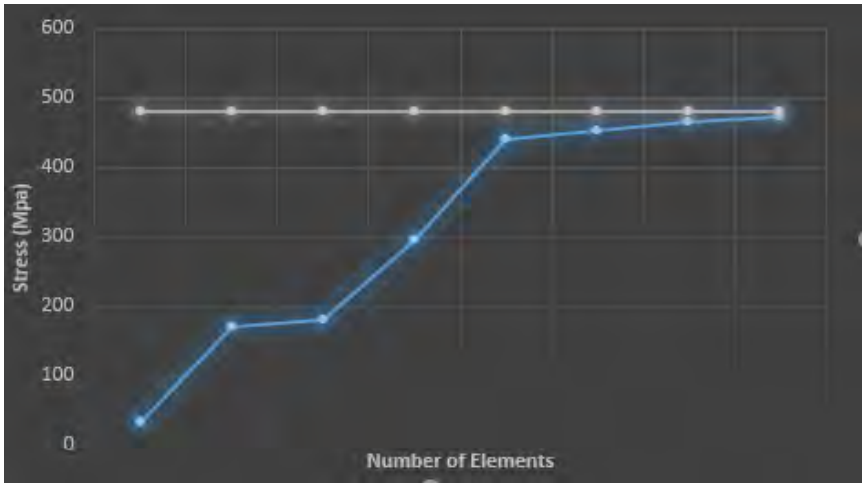

Figure 5.3 Gear contact stress alteration, considering the increase of the number of elements

With grey color the AGMA gear contact stress is represented, equal to **480.17 MPa**, while the FEA contact stress converges to **474.44 MPa.** For the pinion the AGMA gives us, with a poor difference, contact stress equal to **478.62 MPa**, while the FEA comes with the same value of **474.44 MPa**.

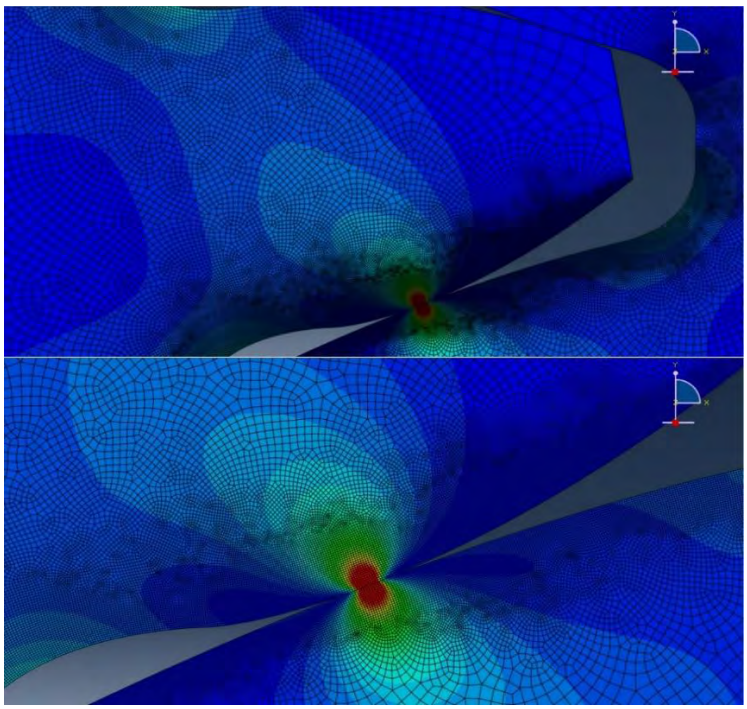

Figure 5.4 Contact stress distribution and location of the maximum

5.2.1 Errors between AGMA and FEA

The procedure followed is the same as the one for the bending stresses, so the AGMA standard is considered as a valid designing method. The errors are as it follows:

	Pinion	Gear
$\sigma_{contact}$(AGMA)	478.62 (MPa)	480.17 (MPa)
$\sigma_{contact}$(FEA)	474.44 (MPa)	474.44 (MPa)
Error	**0.88%**	**1.19%**

Table 5.3 **Error from finite element analyzing for contact stress of pinion and gear**

In the contact designing, AGMA is also stricter, however the error in this case is significantly small. Therefore, the verification of the standard is achieved, using the finite element method.

5.2.2 Safety factors

From the excel file the maximum allowable contact stress for the gear is:

$\boldsymbol{\sigma_{allG} = 912.52}$ $(\boldsymbol{MPa})$ and for the pinion: $\boldsymbol{\sigma_{allP} = 933.52}$ $(\boldsymbol{MPa})$. Both values are below the tensile strength as shown in **Table 4.2**. The safety factors are represented in the **Table 5.4** below.

	AGMA		Finite Element Analysis	
	Pinion	Gear	Pinion	Gear
Safety Factors	**1.91**	**1.94**	**1.97**	**1.92**

Table 5.4 Contact Stress safety factors for AGMA and FE analysis

In this case the safety factors are below 2, however they are above 1 so failure is not a likely scenario.

6 Conclusion

The primary goal of this thesis was to verify the AGMA standard on contact and bending stresses appearing on the teeth of two meshing gears. The verification was accomplished with the use of finite element analysis. The modelling was conducted on ABAQUS as a static model composed by three steps. In the final step the desired stresses are obtained, followed by a comparison between them and the output stresses from AGMA. As seen in ***Table 5.1*** the error obtained for bending stress between the two methods is **7.9%** for the pinion and **1.2%** for the gear. This divergence is due to the assumption made, that the load is applied at the tip of the tooth, thus the bending load reaches its highest picks. In contact stresses, the errors are as seen in **Table 5.3**, for the pinion equal to **0.88%** and for the gear **1.19%.** It is obvious that in contact analysis the results are more satisfying than those in bending, however those deflections are acceptable. In general, AGMA provides us with higher values, so a stricter limitation is obtained, considering the stress analysis.
Eventually, whenever is possible, AGMA standard is preferred, as its accuracy and reliability has been proven in gearboxes designing. Another reason for not selecting FEA is that a lot assumption and simplifications are made in the models, in order to limit the computational cost or to reach convergence. Also, for a decent FEA model, computers with the demanded computational power and qualified engineers are needed, which is viable only for big firms. Nonetheless, there are various fields and cases that AGMA is not applicable, so it is vital that finite element analysis is improved in this particular field.

REFERENCES

[1] **ANSI/AGMA_2101-C95. 1996.** *Fundamental Rating Factors and Calculation Methods for Involute Spur and Helical Gear teeth.* s.l. : ERRATA, 1996.

[2] **Bernard J. Hamrock, Steven R. Schmid, Bo Jacobson. 2004.** *Fundamentals of Machine Elements.* s.l. : McGraw-Hill Science/Engineering/Math, 2004.

[3] **Rexnord Industries, LLC, Gear Group. 1978.** *Failure Analysis Gears-Shafts-Bearings-Seals.* 1978.

[4] **Richard G Budynas, Keith J Nisbett. 2014.** *Shigley's Mechanical Engineering Design.* s.l. : McGraw-Hill Education, 2014.

[5] **Robert C. Juvinall, Kurt M. Marshek. 2013.** *Fundamentals of Machine Component Design.* s.l. : Wiley, 2013.

[6] **Staab, J. A. Collins H.R. Busby G.H. 2009.** *Mechanical Design of Machine Elements and Machines.* s.l. : Wiley, 2009.

[7] **Ugural, Ansel C. 2015.** *Mechanical Design of Machine Components.* s.l. : CRC Press, 2015.

[8] **Seok-ChulHwang[a],Jin-HwanLee[b],Dong-HyungLee[c],Seung-HoHan[a],Kwon-HeeLee[a].** *Contact stress analysis for a pair of mating gears.* 2011

[9] **Andrzej Kawalec, Jerzy Wiktor, Dariusz Ceglarek.** *Comparative Analysis of Tooth-Root Strength Using ISO and AGMA Standards in Spur and Helical Gears with FEM-based Verification,* J. Mech. Des. *Sep 2006*

[10] **Jones, Rhys Gareth (2012)** *The mathematical modelling of gearbox vibration under applied lateral misalignment.* PhD thesis, University of Warwick. 2012

[11] **G.K. Raptis, N.T. Costopoulos, A.G. Papadopulos, D.A. Tsolakis,** *Rating of spur gear strength using photoelasticity and the finite element method,* American Journal of Engineering and Applied Sciences 3 (2010) 222–231

[12] **Dassault Systemes**, *Abaqus analysis user's manual* ver. 6.13 20013

[13] **Ali raad hassan**, "*contact stress analysis of spur gear teeth pair"*. World academy of science, engineering and technology international journal of mechanical, aerospace, industrial, mechatronic and manufacturing engineering vol: 3, no: 10, 2009.

[14] **Sunil Kumar, K.K. Mishra, JatinderMadan**, *Stress analysis of spur gear using fem method, National Conference of Advancements and Futuristic Trends in Mechanical and Material Engineering*, Feb 19- 20.2010

[15] **Vishwjeet V.Ambade, Dr. A.V.Vanalkar and P.R.Gajbhiye,**" *Involute Gear Tooth Contact And Bending Stress Analysis"* International Journal of Computational Engineering Research, vol.3, Issue 8, pp. 30-36, Aug. 2013.

[16] **Ram Krishna Rathore and Abhishek Tiwari,**" *Bending Stress Analysis & Optimization of Spur Gear*" International Journal of Engineering Research and Technology, vol.3, Issue 5, pp. 2044-2049, May. 2014.

[17] **R.A. Hassan,** *Contact stress analysis of spur gear teeth pair***,** World Academy of Science, Engineering and Technology 58 (2009) 611–616.


UNIVERSITY OF THESSALY
FOUNDED 1984